



## Far from home: A multi-analytical approach revealing the journey of an African-born individual to imperial Rome

Kevin Salesses<sup>a,b,\*</sup>, Élise Dufour<sup>c</sup>, Vincent Balter<sup>d</sup>, Robert H. Tykot<sup>e</sup>, Nina Maaranen<sup>f</sup>,  
Maïté Rivollat<sup>b,g</sup>, Arwa Kharobi<sup>b,f</sup>, Marie-France Deguilloux<sup>b</sup>, Marie-Hélène Pemonge<sup>b</sup>,  
Jaroslav Brůžek<sup>b,h</sup>, Dominique Castex<sup>b</sup>

<sup>a</sup> Unit of Anthropology and Human Genetics, Université Libre de Bruxelles, Campus du Solbosch, CP192, Avenue F.D. Roosevelt 50, 1050 Brussels, Belgium

<sup>b</sup> PACEA - De la Préhistoire à l'Actuel: Culture, Environnement et Anthropologie, UMR 5199, Université de Bordeaux, CNRS, Bâtiment B8, allée Geoffroy Saint Hilaire, CS50023, 33615 Pessac Cedex, France

<sup>c</sup> Archéozoologie, Archéobotanique: Sociétés, Pratiques et Environnements, AASPE UMR 7209, Muséum national d'Histoire naturelle, CNRS, CP55, 55 rue Buffon, 75005 Paris, France

<sup>d</sup> Laboratoire de Géologie de Lyon: Terre, Planète, Environnement, UMR 5276 (CNRS, ENS, Université Lyon1), École Normale Supérieure de Lyon, 69364 Lyon Cedex 07, France

<sup>e</sup> Department of Anthropology, University of South Florida, 4202 East Fowler Avenue, SOC107, Tampa, FL 33620, USA

<sup>f</sup> Department of Archaeology and Anthropology, Bournemouth University, Talbot Campus, Poole BH12 5BB, United Kingdom

<sup>g</sup> Department of Archaeogenetics, Max Planck Institute for Science of Human History, Kahlaische Strasse 10, 07745 Jena, Germany

<sup>h</sup> Department of Anthropology and Human Genetics, Faculty of Science, Charles University, Viničná 7, 12844 Praha 2, Czech Republic

### ARTICLE INFO

#### Keywords:

Stable and radiogenic isotopes  
Dental morphology  
Ancient DNA  
Mobility  
Diet  
Roman period

### ABSTRACT

Rome saw its number of foreign individuals increase considerably as the empire expanded. These foreigners arrived as either free persons or slaves from the newly conquered provinces and near-frontier zones and came to influence the whole life of the city. Yet relatively little is known about their life histories. In this study, we bring direct evidence for the first example of an African-born migrant, with an origin beyond the southern imperial border, discovered in Rome. Based on a multi-tissue sampling strategy including molar teeth and mandibular cortical bone, a multi-analytical approach including isotopic ( $\delta^{13}\text{C}$ ,  $\delta^{15}\text{N}$ ,  $\delta^{18}\text{O}$ ,  $\delta^{34}\text{S}$ ,  $^{87}\text{Sr}/^{86}\text{Sr}$ ), dental morphology (geometric morphometrics, nonmetric traits) and ancient DNA (mitochondrial DNA, Y chromosome) analyses allows reconstructing the journey and lifeway patterns of the individual US215/Mand1 buried in the mass grave from the catacombs of Saints Peter and Marcellinus. The successful isotopic and dental morphology analyses suggest that the individual was probably born in the vicinity of the Nile Valley or within the central Sahara Desert. Results also suggest a diachronic change of residence in the area during their early life. The way US215/Mand1 reached Rome is still hypothetical, although it seems likely that the individual could have undergone forced migration as a slave to the capital.

### 1 Introduction

During the last centuries of the Republic and the early ones of the Empire, foreign populations of Rome increased very swiftly and, in many ways, came to influence the whole life of the city. Individuals from

the newly conquered provinces and from the near-frontier zones reached the Imperial capital, and a large part of them arrived as enslaved individuals (Abrecht, 2019; de Ligt and Tacoma, 2016; La Piana, 1927; Noy, 2000). Trans-Saharan slave trade and slave traffic across the southern Egyptian border are well-attested during the 1st-3rd century

\* Corresponding author at: Unit of Anthropology and Human Genetics, Université Libre de Bruxelles, Campus du Solbosch, CP192, Avenue F.D. Roosevelt 50, 1050 Brussels, Belgium.

E-mail addresses: [Kevin.Salesses@ulb.be](mailto:Kevin.Salesses@ulb.be) (K. Salesses), [elise.dufour@mnhn.fr](mailto:elise.dufour@mnhn.fr) (É. Dufour), [vincent.balter@ens-lyon.fr](mailto:vincent.balter@ens-lyon.fr) (V. Balter), [rtkot@usf.edu](mailto:rtkot@usf.edu) (R.H. Tykot), [nmaaranen@bournemouth.ac.uk](mailto:nmaaranen@bournemouth.ac.uk) (N. Maaranen), [maite.rivollat@u-bordeaux.fr](mailto:maite.rivollat@u-bordeaux.fr) (M. Rivollat), [akharobi@bournemouth.ac.uk](mailto:akharobi@bournemouth.ac.uk) (A. Kharobi), [marie-france.deguilloux@u-bordeaux.fr](mailto:marie-france.deguilloux@u-bordeaux.fr) (M.-F. Deguilloux), [marie-helene.pemonge@u-bordeaux.fr](mailto:marie-helene.pemonge@u-bordeaux.fr) (M.-H. Pemonge), [Yaro@seznam.cz](mailto:Yaro@seznam.cz) (J. Brůžek), [dominique.castex@u-bordeaux.fr](mailto:dominique.castex@u-bordeaux.fr) (D. Castex).

<sup>1</sup> ORCID number: 0000-0003-2492-1536.

<https://doi.org/10.1016/j.jasrep.2021.103011>

Received 13 July 2020; Received in revised form 19 March 2021; Accepted 16 April 2021

Available online 29 April 2021

2352-409X/© 2021 Elsevier Ltd. All rights reserved.

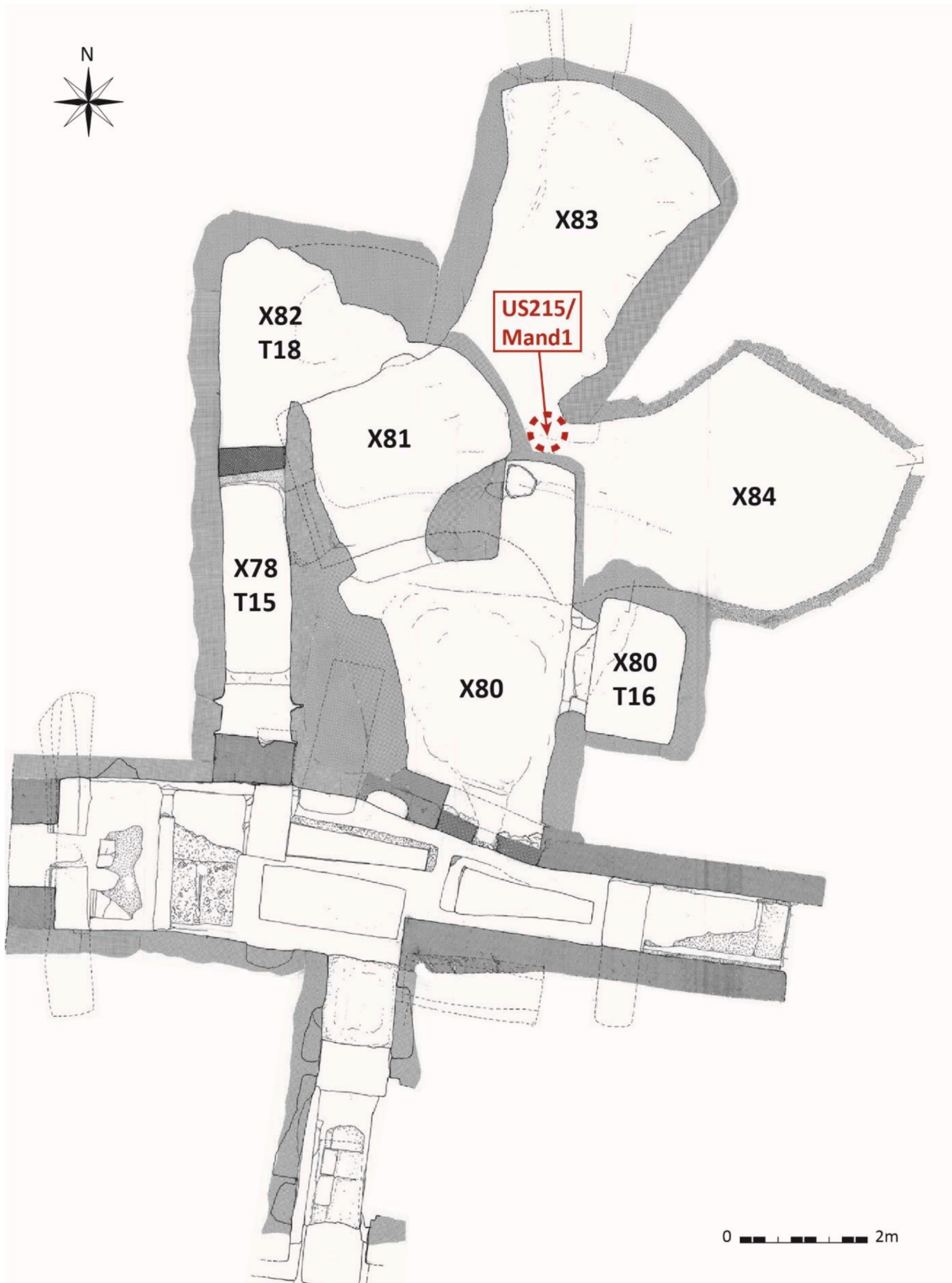


**Fig. 1.** Map of the burial chambers in the SSPM catacombs. Note: The dotted circle indicates the location where the support pillar has been built and US215/Mand1 have been recovered. Modified after M. Ricciardi in [Castex and Blanchard \(2011\)](#).

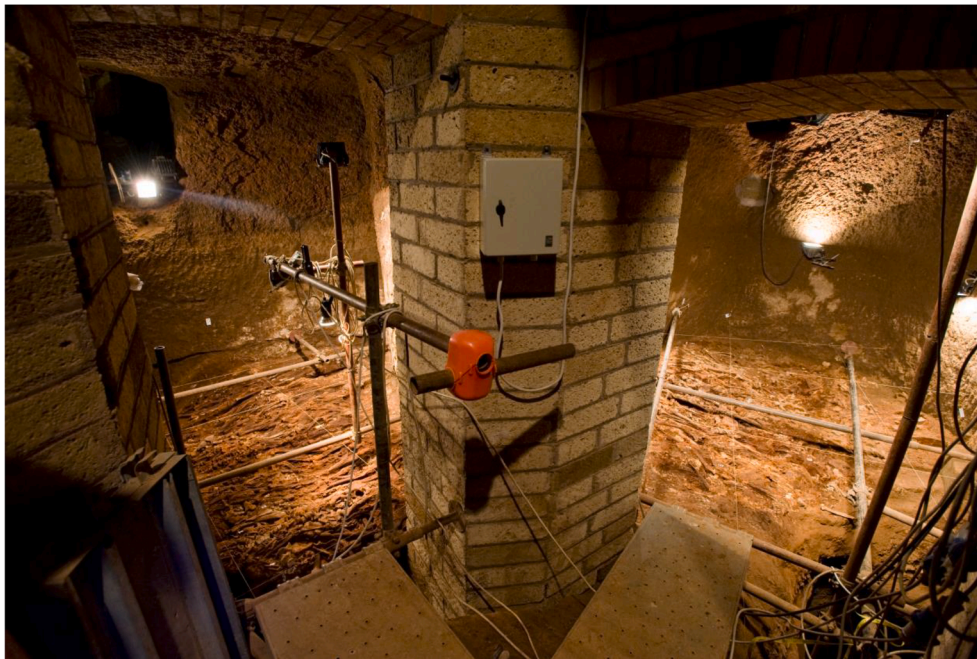


**Fig. 2.** Picture showing the support pillar newly built as well as the burials chambers X83 (left) and X84 (right) in the background. Note: Picture of D. Gliksman/INRAP.

CE, although little evidence is available regarding the scale and the intensity of these imports (Kirwan, 1957; Law, 2009; Snowden, 1947; Wilson, 2012). Ascertaining the number of North African-born slaves and their descendants among the Rome's population is almost impossible, despite the low number often suggested (George, 2003; Tacoma, 2012). Dark-skinned or black Africans were surely a minority among the slave workforce, the majority of which originated from northernmost and easternmost regions of the Roman world (George, 2003; Gordon, 1924; Wilson, 2012). Africans who originated from outside the Empire, like all other slaves in Roman times, may have gained wealth and autonomy as well as achieve a degree of social status (George, 2003). However, most of African-born slaves were exploited in the domestic households of the Roman elite (George, 2003). Romans were fond of exoticism. By exhibiting the possession of such rare slaves, a slave-owner could display a level of sophistication among their *familia* as well as exhibit their wealth and worldliness (George, 2003; McLaughlin, 2014). African slaves could also have served in Rome's armed forces or worked for public institutions or temples (Lenski, 2006; Silver, 2016; Weiss, 2004). Immigration of free men and women must not have been very large in comparison with the importation of slaves. The city of Rome could not attract a large number of foreign workers since most industries already used a servile population. However, the imperial Rome always had a few wholesale merchants, shipowners, bankers, retail traders or adventurers, in pursuit of success, and among them were many foreigners (Abrecht, 2019; de Ligt and Tacoma, 2016; La Piana, 1927; McLaughlin, 2014). Nevertheless, there is, to the best of our knowledge, little indications of such individuals born beyond the southern imperial frontier and established in the capital.

The catacombs of Saints Peter and Marcellinus (hereafter: the SSPM catacombs), located at the third milestone of the ancient Via Labicana, near the modern via Casilina in the south-east of Rome (WGS 84: 41°52'43.4"N 12°32'54.6"E; Precision: exact) is a unique example to further discuss this topic. Among our recent bioarcheological investigations of the SSPM assemblage, one individual, labeled US215/Mand1, drew our attention. Their initial stable oxygen isotope values ( $\delta^{18}\text{O}_{\text{sc}}(\text{enamel})$  up to +2.7‰ – see Results) were very atypical for Rome and suggested a non-European origin, possibly African. The objective of the present work is to refine the life history (dietary patterns, mobility,

geographical origin, and ancestry) of this individual in their population, social and geopolitical contexts, by a multi-analytical approach using additional isotopic measurements on both bone and tooth ( $\delta^{13}\text{C}$ ,  $\delta^{15}\text{N}$ ,  $\delta^{18}\text{O}$ ,  $\delta^{34}\text{S}$ ,  $^{87}\text{Sr}/^{86}\text{Sr}$ ), dental morphology analyses (geometric morphometrics, nonmetric traits) and ancient DNA investigation (mitochondrial DNA, Y chromosome) which are presented here.

## 2 The catacombs of Saints Peter and Marcellinus

In the early 2000s, several mass graves containing circa 3000 skeletons were fortuitously discovered in the oldest part of the SSPM catacombs (i.e. Region X), near the sanctuary of the eponymous saints (Blanchard et al., 2007; Giuliani et al., 2007). The discovered area is characterized by the presence of seven interconnected cavities of various shapes, dimensions and elevations (Fig. 1), and distinct from the other burial chambers (i.e. *cubiculum*) or crypts commonly found in catacomb systems (Blanchard et al., 2007). Archaeological excavations conducted from 2004 to 2010 have made it possible to document the main characteristics of skeletal accumulations and to suspect their relationship with one or more mortality crises (Castex et al., 2007, 2009, 2011). Skeletons were found articulated and placed next to each other or in piles. The new corpses were deposited without disturbing the old ones, and no filling was accumulated among individuals buried in the same level. This evidence in conjunction with the relationship between the capacity of the burial chambers and the volume of the bodies as well as the taphonomic evolution of all the layers of corpses together suggested that several successive multiple inhumations were carried out (Castex et al., 2014; Kacki et al., 2014). The very low frequency (<5%) of traumatic lesions on the assemblage excludes the hypothesis of interpersonal violence as the cause of death (e.g. massacres, martyrdom or human sacrifice) (Castex and Blanchard, 2011). Altogether, the data argue for mortality events of epidemic origin, occurring over a relatively short timeframe (Castex and Blanchard, 2011; Castex et al., 2014). A significant number of the individuals were given highly elaborated funerary practices, never previously recorded in Rome, including the use of gypsum-plastered textiles as body wrappings together with precious and exotic foreign resinous substances (i.e. succinite, sandarac and frankincense) (Devièse et al., 2017; Schotsmans et al., 2019). The high-



Fig. 3. Preserved right hemi-mandible fragment of US215/Mand1.

Table 1

Individuals used in the biodistance (based on dental traits (DT)), geometric morphometrics (GM) and DNA analyses.

DT ID	GM ID	DNA ID	Room/Site	Individual	Sex	Age
–	–	1	X81	n°13/Mand1	U	11.8+
–	1	–	X81	n°14/Mand2	U	16.4+
101	–	–	X81	n°15/Mand2	U	–
102	–	–	X81	n°16/Mand2	U	11.8+
–	–	2	X83	Sq108	F	15–19
203	–	–	X83	Sq093 = 113 = 115	U	20+
204	–	3	X83	Sq152	U	20+
205	–	–	X83	US212/Mand1	U	8.7+
206	2	4	X83	US215/Mand1	U	16.4+
207	–	–	X83	US215/Mand2	U	16.4+
208	–	–	X83	US215/Mand3	U	16.4+
209	–	–	X83	US216/Mand1	U	14.8+
210	3	–	X83	US216/Mand2	U	16.4+
211	4	–	X83	US217/Mand1	U	16.4+
212	5	5	X83	US219/Mand1	U	16.4+
–	–	6	X83	US219/Mand2	U	11.8+
313	–	–	X84	Sq187	F?	15–19

level care offered to the deceased as well as the presence of good-to-high quality textile remains (e.g. gold and probable silk threads, fineness of the weave) suggested that at least part of these individuals belonged to the upper classes of the Roman society (Blanchard et al., 2015; Devière et al., 2017). Analysis of grave goods and  $^{14}\text{C}$  data revealed that the mass graves dated back to the early imperial period (1st–3rd c. AD) (Blanchard et al., 2015; Castex and Blanchard, 2011).

### 3 Material

The individual US215/Mand1 was found in the chamber X83 during a rescue survey conducted prior to the construction of a support pillar to secure the site (Fig. 2). Time limitation as well as structural instability constrained investigators to remove human remains rapidly in layers of 20 cm in thickness at this location. In the prospect of a large-scale isotopic study in the SSPM catacombs, a minimum number of individuals of 14 based on right hemi-mandibles with at least the second molar embedded was estimated on this assemblage (Salessé, 2015). Among them was US215/Mand1, represented by only three lower right

permanent molars in the mandible fragment (Fig. 3).

Enamel of all teeth as well as a piece of mandibular cortical bone were sampled to isotopically investigate diet and mobility of US215/Mand1. This multi-tissue sampling strategy allows exploiting the differential growth timing of skeletal elements in order to reconstruct a detailed life history, at the scale of the individual (see Supplementary File A). The isotopic results from US215/Mand1 have been compared to those of the rest of the corpus ( $n = 129$  individuals) from the Region X mass graves (Salessé, 2015) and then have been geographically recontextualized by comparisons with animal and human populations from Italy or beyond (Buzon and Simonetti, 2013; di Lernia et al., 2013; Killgrove and Tykot, 2013, 2018; Nitsch, 2012; O’Connell et al., 2019; Prowse et al., 2004; Rutgers et al., 2009; Schrader et al., 2019; Sereno et al., 2008; Tafuri et al., 2006, 2018).

A small dataset (right-side mandible fragments with molars) from the mass graves of the catacombs ( $n = 13$ , including US215/Mand1; Table 1), available at the time of this study, have been used to explore biodistance through dental nonmetric traits. Further exploration of molar outline shape was conducted on US215/Mand1 and a subset of individuals from the SSPM catacombs ( $n = 4$ , Table 1) using geometric morphometrics.

Dentine of the US215/Mand1’s second molar has been sampled for exploring the paternal and maternal lineages through ancient DNA analysis. Teeth of a small batch of individuals ( $n = 5$ , Table 1) randomly selected in the mass graves of the catacombs have also been investigated for comparative purposes.

### 4 Methods

The principles of the stable isotope analysis (including abbreviations), the dental morphology study and the paleogenetic approach are set out in Supplementary File A.

#### 4.1. Isotopic analysis

##### 4.1.1. Bone collagen extraction for $\delta^{13}\text{C}$ , $\delta^{15}\text{N}$ , and $\delta^{34}\text{S}$ analyses

Bone preparation and chemical pretreatments were conducted at the stable isotope preparation lab of UMR 7209 in the *Muséum National d’Histoire Naturelle* (MNHN) (Paris, France). Sampled bones were cleaned using a tungsten carbide drill bit to retain only compact parts.

Bone collagen was extracted following the protocol of Longin (1971), modified by Bocherens et al. (1988) and Bocherens et al. (1991). Bones were crushed using a knife mill or a mortar and pestle. Powder samples (amount:  $\approx 400$  mg; grain size: 0.3–0.7 mm) were decalcified in 40 ml of 1 M hydrochloric acid (HCl) at room temperature for 20 min. Gelatins were retrieved by filtration using a MF-Millipore membrane filter (pore size: 5  $\mu\text{m}$ ), rinsed, and then soaked into 0.125 M sodium hydroxide at room temperature for 20 h to remove soil organic matter. The samples were again filtered and rinsed. Gelatins were solubilized in 0.01 M HCl ( $\text{pH} = 10^{-2}$ ) at 100 °C for 17 h and filtered a last time to trap possible impurities. Collagen samples were freeze-dried at  $-87$  °C for at least 48 h and extraction yields (%Col) were calculated (expressed as a weight percentage, wt%). In modern bones, extraction yields are around  $20.4 \pm 3.9$  wt% (1SD) (Bocherens et al., 1991; Salessé et al., 2019), and samples containing  $< 1$  wt% of collagen are considered unreliable (Dobberstein et al., 2009; Van Klinken, 1999).

Carbon and nitrogen abundances and isotope compositions were measured (amount: 200–400  $\mu\text{g}$ ) using a Costech Elemental Analyzer 4010 fitted with a zero-blank auto-sampler coupled via a ConFlo IV to a ThermoScientific Delta V PLUS Isotope Ratio Mass Spectrometer at the environmental isotope laboratory of the James Cook University's advanced analytical center (Cairns, Australia). Carbon and nitrogen contents are expressed as percentages (%C and %N). In modern bones, %C and %N values range from 15.3 to 47% and from 5.5 to 17.3%, respectively (Ambrose, 1990; Salessé et al., 2019). Samples with %C and %N values below 13% and 4.8%, respectively, are recognized as severely altered (Ambrose, 1990; Garvie-Lok, 2001; Iacumin et al., 1998; Reitsema, 2012; Van Klinken, 1999). Atomic C:N ratios of modern bones vary between 2.9 and 3.6 (DeNiro, 1985; Salessé et al., 2019), and archaeological samples with values below or above these thresholds indicate alteration or contamination. The  $\delta^{13}\text{C}_{\text{col}}$  and  $\delta^{15}\text{N}_{\text{col}}$  values are reported as per mil (‰) difference relative to VPDB and AIR, respectively. International and in-house standards (USGS-40:  $\delta^{13}\text{C} = -26.4\text{‰}$  and  $\delta^{15}\text{N} = -4.5\text{‰}$ ; Taipan:  $\delta^{13}\text{C} = -11.7\text{‰}$  and  $\delta^{15}\text{N} = 11.8\text{‰}$ ; Chitin:  $\delta^{13}\text{C} = -19\text{‰}$  and  $\delta^{15}\text{N} = 2.2\text{‰}$ ) were analyzed for quality control. During this study, analytical errors calculated from replicates of internal standards were better than  $\pm 5\%$  (1SD) for both %C and %N,  $\pm 0.1\%$  (1SD) for  $\delta^{13}\text{C}_{\text{col}}$  and  $\pm 0.2\%$  (1SD) for  $\delta^{15}\text{N}_{\text{col}}$ .

Sulfur abundance and isotope composition were assessed (amount: 7–8 mg) using a Costech Elemental Analyzer 4010 coupled with a ThermoScientific Delta V Advantage isotope ratio mass spectrometer at the University of South Florida Stable Isotope Lab (Tampa, Florida, USA). Sulfur content is expressed in percentages (%S). In modern bones, %S values as well as the atomic C:S and N:S ratios range from 0.15 to 0.35%, from 300 to 900, and from 100 to 300, respectively (Bocherens et al., 2011; Nehlich and Richards, 2009). Bone collagen samples with values outside these ranges are considered unreliable. The  $\delta^{34}\text{S}$  results are reported as per mil (‰) deviation and normalized to CDT using certified and in-house reference materials (IAEA-S2:  $\delta^{34}\text{S} = 22.7\text{‰}$ ; IAEA-S3:  $\delta^{34}\text{S} = -32.3\text{‰}$ ; and Elemental Microanalysis B2155:  $\delta^{34}\text{S} = 6.7\text{‰}$ ). Measurements errors calculated from 46 replicates of the B2155 standard were  $\pm 0.11\%$  (1SD) for %S and  $\pm 0.36\%$  (1SD) for  $\delta^{34}\text{S}_{\text{col}}$ .

#### 4.1.2. Bone and tooth carbonate preparation for $\delta^{13}\text{C}$ and $\delta^{18}\text{O}$ analyses

Bone carbonate preservation was investigated by Fourier transform infrared (FTIR) spectroscopy in attenuated total reflection (ATR) mode before pretreatments (see Lebon et al., 2011; Salessé et al., 2014 for a presentation of the protocol used). The diagenetic trajectory of bone samples from the SSPM catacombs has already been described in Salessé et al. (2014).

Bone and tooth carbonate samples were prepared following a revised version proposed by Salessé et al. (2013) of the protocol of Balasse et al. (2002) at the MNHN. Sampled bones were crushed as described above. Selected teeth were first cleaned and then sampled over the entire height of the crown with a tungsten carbide drill bit. Powder samples (amount:  $\approx 30$  mg; grain size  $< 0.3$  mm) were treated with 1.5 ml of 2–3% sodium

hypochlorite (NaClO) at room temperature for 48 h to remove organic matter, and then with 1.5 ml of 1 M acetic acid ( $\text{CH}_3\text{COOH}$ ) at room temperature for 1 h to remove exogenous carbonates. NaClO and  $\text{CH}_3\text{COOH}$  solutions were renewed at least once during the procedure. Samples were rinsed with distilled water between the two steps and at the end. Samples were oven-dried at 65 °C overnight. The purification process induced significant weight losses, up to 80%.

Carbon and oxygen isotope compositions were measured (amount: 580–630  $\mu\text{g}$ ) via a ThermoScientific Kiel IV carbonate device interfaced with a ThermoScientific Delta V Advantage isotope ratio mass spectrometer at the MNHN's isotope-ratio mass spectrometry service. The results are reported as per mil (‰) deviation from VPDB reference standard scale. An in-house carbonate standard (Marble LM:  $\delta^{13}\text{C} = 2.13\text{‰}$  and  $\delta^{18}\text{O} = -1.83\text{‰}$ ), normalized to the international standard NBS 19, was used for checking the accuracy of the measurements. Analytical precision calculated from 107 replicates of Marble LM were  $\pm 0.03\text{‰}$  (1SD) for  $\delta^{13}\text{C}$  and  $\pm 0.07\text{‰}$  (1SD) for  $\delta^{18}\text{O}$ .

#### 4.1.3. Tooth enamel sample preparation for $^{87}\text{Sr}/^{86}\text{Sr}$ analysis

Samples were processed in a clean room with filtered air and under laminar-flow hoods at the *École Normale Supérieure* (ENS) (Lyon, France). Enamel samples were prepared as mentioned above. Powder samples (amount:  $\approx 30$  mg; grain size  $< 0.3$  mm) were ultrasonicated in 1 ml of 0.1 M  $\text{CH}_3\text{COOH}$  for 5 min to eliminate diagenetic carbonates, rinsed with MilliQ water to neutral, and then freeze-dried at  $-50$  °C for at least 12 h. Samples were then dissolved in 1 ml of 4 M of nitric acid ( $\text{HNO}_3$ ). An aliquot of 100  $\mu\text{l}$  was taken from each sample for trace element concentration analysis.

Strontium was isolated following a similar protocol to that described in De Muynck et al. (2009). Teflon ion exchange columns were filled with 2 ml of 50–100  $\mu\text{m}$  bead size TrisKem Sr-Resin. Resin was washed with MilliQ water and 0.05 M  $\text{HNO}_3$ , and then pre-conditioned with 3 ml of 4 M  $\text{HNO}_3$ . The dissolved samples were loaded into the columns. Column blanks were prepared with 1 ml of 4 M  $\text{HNO}_3$ . Columns with samples were rinsed with 5 ml of 4 M  $\text{HNO}_3$  to remove concomitant matrix elements, and then with 6 ml of 0.05 M  $\text{HNO}_3$  to strip off the purified strontium fraction. Retrieved strontium samples were evaporated, and dried residues were finally dissolved in 1 ml of 0.05 M  $\text{HNO}_3$ .

Strontium concentrations were determined using an Agilent 7500 CX inductively coupled plasma mass spectrometry following the method of Balter and Lécuyer (2010), whereas strontium isotope ratios were measured using a large-radius Nu 1700 multi-collector inductively coupled plasma mass spectrometer, both at the ENS. Strontium isotope data were obtained at low-resolution in static mode. Signal intensities were monitored on  $^{83}\text{Kr}$  and  $^{85}\text{Rb}$  and used to correct for interferences on  $m/z$  ratios of 84 (Kr), 86 (Kr), and 87 (Rb). Ratios were corrected for mass bias fractionation using an internal normalization to  $^{86}\text{Sr}/^{88}\text{Sr} = 0.1194$ . Gas flow instrumental mass fractionation was controlled with a standard-sample bracketing approach involving the measurement of the standard NIST SRM 987 (recommended value of  $^{87}\text{Sr}/^{86}\text{Sr} = 0.710248$ ; McArthur, 2001). Samples were randomized during analysis and duplicates were measured to check for systematic errors. Repeated measurements of NIST SRM 987 standard yielded an average value of  $^{87}\text{Sr}/^{86}\text{Sr} = 0.71025 \pm 0.00002$  (2SD; 12 analyses).

#### 4.1.4. Isotopic data processing

The Bayesian model FRUITS (Food Reconstruction Using Isotopic Transferred Signals, version 2.1.1; Fernandes et al., 2014) was applied to evaluate the relative importance of plant and animal resources in the US215/Mand1's diet as well as estimate their protein and carbohydrate/fat intakes. The model parameters used are detailed in the Supplementary File B.

To reconstruct the  $\delta^{18}\text{O}_{\text{dw}}(\text{enamel})$  values of US215/Mand1, three steps were followed: 1) converting  $\delta^{18}\text{O}_{\text{sc}}[\text{VPDB}]$  into  $\delta^{18}\text{O}_{\text{sc}}[\text{VSMOW}]$  values using the equation of Coplen (1988) (Eq. (1)); 2) estimating  $\delta^{18}\text{O}_{\text{phosphate}}[\text{VSMOW}]$  from  $\delta^{18}\text{O}_{\text{sc}}[\text{VSMOW}]$  values via the equation

**Table 2**  
Traits used to investigate biodistance.

Trait	Abbr.	Tooth	Reference	Type	n
Protostylid	PR	LM1	Scott and Irish, 2017	Binary	5
Deflecting wrinkle	DW	LM1	Scott and Irish, 2017	Ordinal	9
Hypoconulid	C5	LM2	Scott and Irish, 2017	Ordinal	10
Groove pattern (present = y)	GP	LM2	Scott and Irish, 2017	Binary	13
Anterior fossa	AF	LM2	Scott and Irish, 2017	Ordinal	12
Enamel extension	EE	LM2	Scott and Irish, 2017	Ordinal	13
Root number	R	LM2	Scott and Irish, 2017	Ordinal	8
Crenulation	C	LM2	Pilloud et al., 2018	Binary	8
Lower third molar absence	UM3V	LM3	Scott and Irish, 2017	Binary	12
Mandibular molar pit tubercle	MPT	LM3	Marado and Silva, 2016	Ordinal	8
Torsomolar angle	TA	LM3	Scott and Irish, 2017	Binary	9

Note: 'Abbr.' stands for abbreviation. 'Tooth' refers to teeth selected to represent the trait. 'Type' refers to the way the trait was coded into the software. 'n' indicates the overall number of observations from the SSPM individuals.

developed by Chenery et al. (2012) (Eq. (2)); and 3) calculating  $\delta^{18}\text{O}_{\text{dw}}$  [VSMOW] from  $\delta^{18}\text{O}_{\text{phosphate}}$  [VSMOW] values thanks to the formula proposed by Daux et al. (2008) (Eq. (3)).

$$[\delta^{18}\text{O}_{\text{sc}} \text{ [VSMOW]} = 1.03091 \times \delta^{18}\text{O}_{\text{sc}} \text{ [VPDB]} + 30.91] \quad (1)$$

$$[\delta^{18}\text{O}_{\text{phosphate}} \text{ [VSMOW]} = 1.122 \times \delta^{18}\text{O}_{\text{sc}} \text{ [VSMOW]} - 13.73] \quad (2)$$

$$[\delta^{18}\text{O}_{\text{dw}} \text{ [VSMOW]} = 1.54 \times \delta^{18}\text{O}_{\text{phosphate}} \text{ [VSMOW]} - 33.72] \quad (3)$$

To reconstruct the  $\delta^{18}\text{O}_{\text{dw}}$  (bone) values of US215/Mand1, two steps were followed: 1) converting  $\delta^{18}\text{O}_{\text{sc}}$  [VPDB] into  $\delta^{18}\text{O}_{\text{sc}}$  [VSMOW] values using the equation of Coplen (1988) (Eq. (1)); and 2) calculating  $\delta^{18}\text{O}_{\text{dw}}$  [VSMOW] from  $\delta^{18}\text{O}_{\text{sc}}$  [VSMOW] via the equation proposed by Chenery et al. (2012) (Eq. (4)).

$$\delta^{18}\text{O}_{\text{dw}} \text{ [VSMOW]} = 1,59 \times \delta^{18}\text{O}_{\text{sc}} \text{ [VSMOW]} - 48,634. \quad (4)$$

These two procedures are recommended by Chenery et al. (2012) for individuals originating from geographical regions characterized by a hot-arid climate and for individuals originating from the rest of the world, respectively.

Finally, all the isotopic data, together with associated chronological and other supporting information, from this study have been uploaded in the IsoArch database (Salessé et al., 2018, 2020).

## 4.2. Dental morphology analysis

### 4.2.1. Nonmetric traits

Dental traits (see list in Table 2) were recorded either as present/absent or as a grade from absent to full expression, following the appropriate guidelines (i.e. Marado and Silva, 2016; Pilloud et al., 2018; Scott and Irish, 2017). An interesting dental nonmetric trait, crenulation, was included in the investigation. The trait is currently not part of the ASUDAS but has recently been explored further by Pilloud et al. (2018) who observed highest frequencies (and scores) for the trait among modern American Black and South African samples.

As recommended, each trait was represented by one tooth in the final analysis to prevent redundancy (Irish, 2005; Nichol, 1990). To analyze the dental nonmetric data, a distance matrix was created using Gower distances which measures the distance between pairs and then combines the distances into a single value per record-pair (Gower, 1971). This allows for missing data and the use of a mixed dataset of interval, ordinal

and categorical data. However, the generated distance matrix is non-Euclidean, requiring nonparametric tools for further data analysis. The distance matrix was created using the function daisy in R package cluster (Maechler et al., 2019), allowing the user to define symmetric and asymmetric binary values (e.g. in the case of rare traits). The morphological similarities were further analyzed using the function pam in cluster, which partitions the data into clusters around medoids represented by individual datapoints. Data was visualized using nonmetric multidimensional scaling (NMDS) and t-distributed Stochastic Neighbor Embedding (t-SNE). Both are dimension reduction techniques intended to condense data to a visually observable form. The former is a built-in statistical tool in R (R Core Team, 2020), the latter was created using the R package Rtsne (van der Maaten and Hinton, 2008).

### 4.2.2. Geometric morphometrics

Geometric morphometrics was utilized to explore shape change between a subset of individuals, with the individual of interest as reference. To investigate only the shape of organism, size, location and orientation must be excluded from the coordinates. The most common method to do this is the generalized Procrustes superimposition where landmarks are rotated to best fit, centered and rescaled to a size 1 (Webster and Sheets, 2010). The coordinates exist in Kendall's shape space (Kendall, 1984), defined as a mathematical space induced by the shape coordinates (Mitteroecker and Gunz, 2009). To treat the semi-landmarks, bending energy (Bookstein, 1997) which maps the 'path of least resistance' between neighboring landmarks, was used.

The mandible fragments were digitized using the R package Stereomorph (Olsen and Westneat, 2015), which created shape files for each sample, and analyzed with the sibling package geomorph (Collyer and Adams, 2018). Due to attrition on the occlusal surfaces (and the subsequent loss of landmark information), the analysis was constricted to an investigation of the outline created by the three molars, using two landmarks as anchor and semi-landmarks to map the outline. The landmarks were used only momentarily, the analysis focusing on semi-landmark-based outline due to heavy wear, as Stereomorph requires them to create a start and end point for the semi-landmarks. To make sure the outline resembles the tooth shape as well as possible, the landmarks were placed at the meeting point of cusp 3 and 5 on LM1, as close to one another as possible, while the semi-landmarks were placed around the tooth in the same direction. Before connecting the semi-landmarks, they were redistributed around the shape in even distances using the package function lapply. Because we wanted to create a closed outline of the three molars, the landmarks were omitted from the outline to avoid duplication of the points (landmarks would correlate with the first and last semi-landmark along the curve). Generalized Procrustes superimposition was then performed using function gpgen. The differences between individuals were visualized using functions plotTangentSpace, performing PCA, and plotRefToTarget which place the configuration on a grid and deforms it in locations where change is observed.

### 4.3. aDNA extraction and analysis

Ancient DNA (aDNA) analyses were not anticipated before the excavation. The teeth were therefore decontaminated, i.e. scraped, cleaned with bleach, and subsequently exposed to UV radiation for 20 min on each side. All established aDNA guidelines were then followed to minimize contamination during subsequent steps. Analyses were conducted in the aDNA facilities of UMR PACEA at Bordeaux University (Pessac, France). The teeth were powdered and a sample of 100 mg for each was incubated overnight in lysis buffer (0.5 M EDTA, pH 8, 25 mg/ml proteinase K, and 0.5% N-Lauryl sarkosyl). The procedure of Allen-toft et al. 2015 was then followed to extract the DNA (MinElute kit, Qiagen). In order to assess maternal (mitochondrial DNA) and paternal (Y chromosome) lineages, a combination of 18 mitochondrial and 10 Y chromosome SNPs were typed through one multiplex using MALDI-TOF

**Table 3**  
Stable isotope results for reconstruction dietary patterns of US215/Mand1.

US215/Mand1 - Diet													
Molar teeth			Mandibular bone										
M1	M2	M3	%Col	%C	%N	%S	C:N	C:S	N:S	$\delta^{13}\text{C}_{\text{col}}$	$\delta^{15}\text{N}_{\text{col}}$	$\delta^{34}\text{S}_{\text{col}}$	$\delta^{13}\text{C}_{\text{carb}}$
$\delta^{13}\text{C}_{\text{carb}}$	$\delta^{13}\text{C}_{\text{carb}}$	$\delta^{13}\text{C}_{\text{carb}}$											
-12.9	-12.5	-12.3	6.7	38.5	13.6	0.31	3.3	331.2	100.3	-19.0	+12.5	+8.4	-13.9

**Table 4**  
Stable isotope results for discussing the mobility of US215/Mand1.

US215/Mand1 - Mobility											
Molar teeth						Mandibular bone					
M1			M2			M3					
$\delta^{18}\text{O}_{\text{carb}}$	$\delta^{18}\text{O}_{\text{dw}}$	$^{87}\text{Sr}/^{86}\text{Sr}$	$\delta^{18}\text{O}_{\text{carb}}$	$\delta^{18}\text{O}_{\text{dw}}$	$^{87}\text{Sr}/^{86}\text{Sr}$	$\delta^{18}\text{O}_{\text{carb}}$	$\delta^{18}\text{O}_{\text{dw}}$	$^{87}\text{Sr}/^{86}\text{Sr}$	$\delta^{18}\text{O}_{\text{carb}}$	$\delta^{18}\text{O}_{\text{dw}}$	
+1.3	+0.9	0.7085	+2.3	+2.6	0.7086	+1.2	+0.7	0.7087	-3.0	-4.4	

Note: See section 4.1.4 for the conversion procedures to estimate the  $\delta^{18}\text{O}_{\text{dw}}$  values.

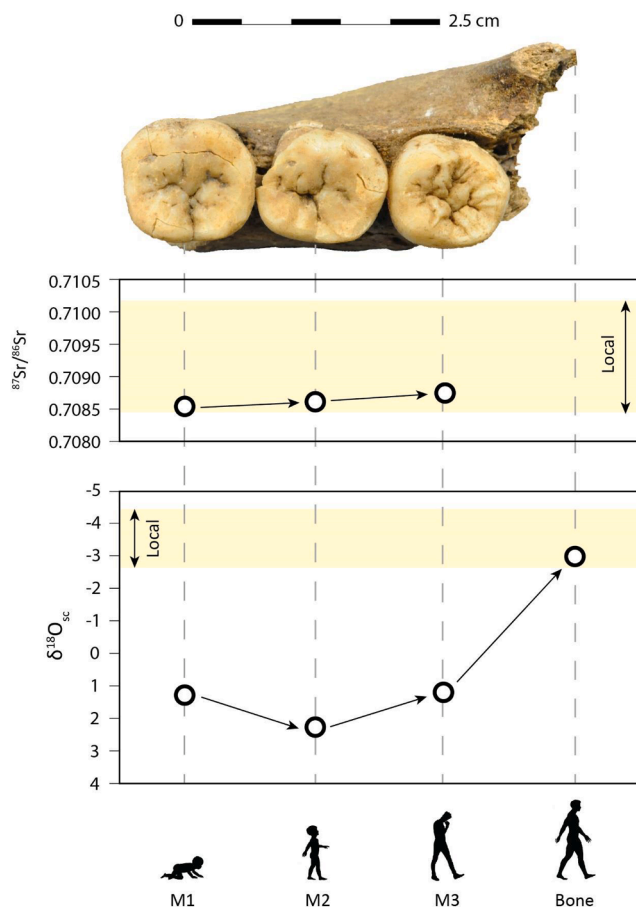


**Fig. 4.** Variation of the  $^{87}\text{Sr}/^{86}\text{Sr}_{\text{enamel}}$ ,  $\delta^{18}\text{O}_{\text{sc}}(\text{enamel})$  and  $\delta^{18}\text{O}_{\text{sc}}(\text{bone})$  values in US215/Mand1. Note: 'M1', 'M2' and 'M3' stands for permanent molars 1, 2 and 3, respectively. The yellow area corresponds to the local range defined as one standard deviation from the SSPM population mean. The standard deviation between replicates is inferior to size of dots.

MS-based SNP genotyping (iPLEXTM Gold technology, Sequenom, Inc., San Diego, CA, USA). All primers used for these experiments and procedure details are available in Rivollat et al. (2015). This first set of analyses was also designed to test for the ancient DNA conservation in the human remain and, in case of sufficient DNA preservation, was

supposed to be followed by the characterization of the mitochondrial first hypervariable region (HVR-I, nps 16,024–16,380) targeted using four overlapping fragments (following the procedures described in Rivollat et al., 2015).

## 5 Results

### 5.1. Mobility and dietary patterns of US215/Mand1 through stable isotopic data

Collagen was successfully extracted from the mandibular fragment of US215/Mand1. With an extraction yield of 6.7 wt%, it exceeds the minimum threshold of 1 wt% indicating a satisfactory sample preservation (Table 3). With 38.5%, 13.6% and 0.31% respectively, carbon, nitrogen and sulfur contents fall into the reference ranges for well-preserved collagen samples (Table 3). The atomic C:N, C:S and N:S ratios are 3.3, 331.2 and 100.3 respectively, which is well within the acceptable ranges of variation for unaltered and uncontaminated collagen samples (Table 3). Therefore, the collagen extract of this individual meets all the criteria for good-quality collagen. Regarding the FTIR indicators for bone carbonate preservation, the mandible fragment of US215/Mand1 presents an IRSF value of 4.1, a  $\text{CO}_3/\text{PO}_4$  ratio of 0.46 and an Amide I/ $\text{PO}_4$  ratio of 0.24. These values differ significantly from those measured on modern reference samples (see Saless et al., 2014 and references therein). Compared to the rest of the population (Saless et al., 2014), US215/Mand1 falls into the group of bones moderately recrystallized. It was, however, demonstrated that samples falling in this group had reliable carbonate isotope signals (Saless et al., 2014). Tooth preservation was not investigated since it is widely recognized that enamel can survive most diagenetic regimes and preserve biogenic isotopic signals, especially in European archaeological contexts as young as the Roman ones (e.g. Koch et al., 1997; Wang and Cerling, 1994; Zazzo, 2014). The isotopic results obtained in this study can therefore be considered reliable and used to explore mobility and diet.

US215/Mand1 exhibits  $^{87}\text{Sr}/^{86}\text{Sr}_{\text{enamel}}$  ratios of 0.7085, 0.7086 and 0.7087 for M1, M2 and M3, respectively (Table 4; Fig. 4). These  $^{87}\text{Sr}/^{86}\text{Sr}_{\text{enamel}}$  ratios are within one standard deviation from both the SSPM and the other Lazio population means (Figs. 4 and 5). Further, US215/Mand1 presents  $\delta^{18}\text{O}_{\text{sc}}(\text{enamel})$  values of +1.3‰, +2.3‰ and +1.2‰ for M1, M2 and M3, respectively (Table 4). These  $\delta^{18}\text{O}_{\text{sc}}(\text{enamel})$  values are significantly higher than the rest of the population from the region X of the SSPM catacombs (Grubb's tests;  $p < 0.00$ ) (Fig. 4), and other Roman individuals from Lazio (Grubb's tests;  $p < 0.00$ ) (Fig. 6). In contrast, with a  $\delta^{18}\text{O}_{\text{sc}}(\text{bone})$  value of -3.0‰ (Table 4), US215/Mand1 lies within one standard deviation from the population mean (Fig. 4).

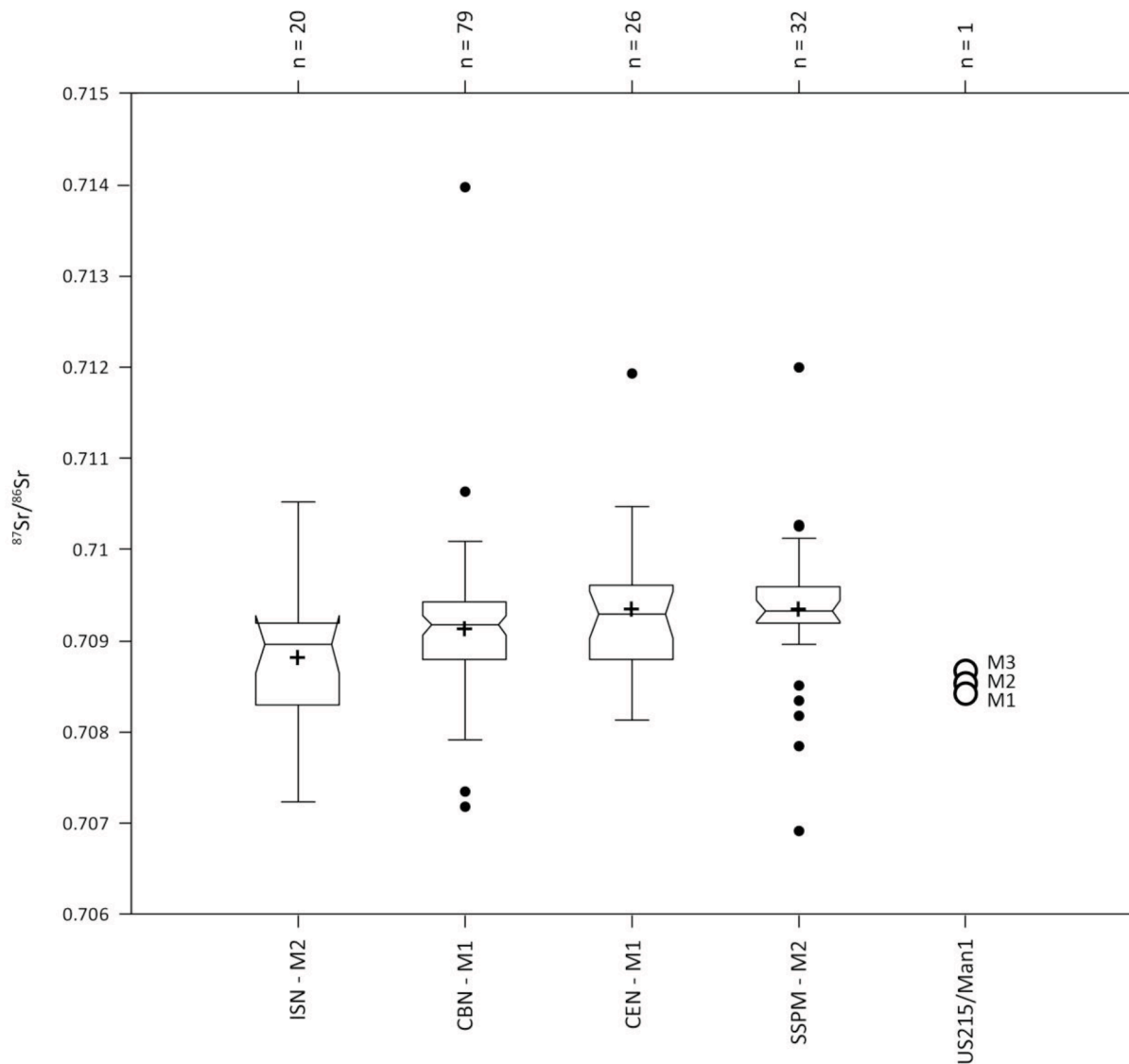


**Fig. 5.** Inter-site comparison of the  $^{87}\text{Sr}/^{86}\text{Sr}$  ratios measured on human dental samples from the Rome's region. Note: 'M1' and 'M2' stands for permanent molars 1 and 2, respectively. 'ISN' refers to Isola Sacra Necropolis, 'CBN' to Casal Bertone Necropolis, 'CEN' to Castellaccio Europarco Necropolis, and 'SSPM' to Saints Peter and Marcellinus catacombs. Bibliographic references: Salessé (2015), Killgrove and Montgomery (2016), Stark (2017). The boxes depict groups of data through their quartiles.

The estimated  $\delta^{18}\text{O}_{\text{dw}}$  values of US215/Mand1 vary between +0.7‰ and +2.6‰ on teeth and it is +4.4‰ on bone (Table 4).

Breastfeeding and weaning could theoretically explain the high  $\delta^{18}\text{O}_{\text{sc (enamel)}}$  values of US215/Mand1. Breast milk is enriched in  $^{18}\text{O}$  over the consumed drinking water, inducing elevated  $\delta^{18}\text{O}$  in infant tissues (Britton et al., 2015). Among modern humans living in non-industrialized and traditional fertility societies, cessation of breastfeeding occurs in most cases between the age of two or three (Alvarez, 2000; Britton et al., 2015; Kennedy, 2005; Sellen, 2001, 2007). Such a pattern was also identified in Roman populations over the Empire based on isotopic but also written evidence (for Rome, see Prowse et al., 2008; for Africa, see Dupras et al., 2001; Keenleyside et al., 2009). Among teeth, only permanent first molars have their crown mineralized between birth and the age of three; the other molars covering posterior age periods (Moorrees et al., 1963). Thus, breastfeeding processes affect commonly only isotopic signals of M1s. These effects are, however, relatively limited, and lead to an increase of  $\delta^{18}\text{O}_{\text{sc (enamel)}}$  by approximately +0.7‰ (Herring et al., 1998; Knudson, 2009; Roberts et al., 1988; Wright and Schwarcz, 1998, 1999). US215/Mand1 has a lower  $\delta^{18}\text{O}_{\text{sc (enamel)}}$  value on M1 than on M2 (Fig. 4), which is an opposite

pattern to what one can expect in case of a consumption of breast milk and then a weaning during the first years of life. Moreover, US215/Mand1 M1 exhibits a far higher value than the other SSPM population M2s (mean =  $-3.7 \pm 1.1\text{‰}$ ) (Fig. 6). The  $\delta^{18}\text{O}_{\text{sc (enamel)}}$  difference between US215/Mand1 M1 and the SSPM population M2s is 5‰, and greatly exceeds the mean  $^{18}\text{O}$ -enrichment of M1s caused by nursing.

Food and beverage processing could have influenced the  $\delta^{18}\text{O}_{\text{sc}}$  signals recorded in US215/Mand1 enamel samples. Culture-specific culinary and dietary practices can be responsible of sizeable modifications of the original stable isotope compositions of water in food and beverages (Brettell et al., 2012; Britton et al., 2015; Daux et al., 2008; Warinner and Tuross, 2009). Recent experiments highlighted that specific cooking processes may shift the  $\delta^{18}\text{O}$  values of food resources up to +5.2‰ (e.g. Royer et al., 2017). In a lower degree, beverage production techniques and storage may increase the  $\delta^{18}\text{O}$  values of the initially used water up to +1.3‰ (e.g. Brettell et al., 2012; Spangenberg and Venemann, 2008). If food water and drinking liquids contribute together to the final oxygen isotopic composition of consumer's body tissues, the former contributes much less than the latter to this signal. Thus, the shifted  $\delta^{18}\text{O}$  values of food would be mitigated by those of beverages.



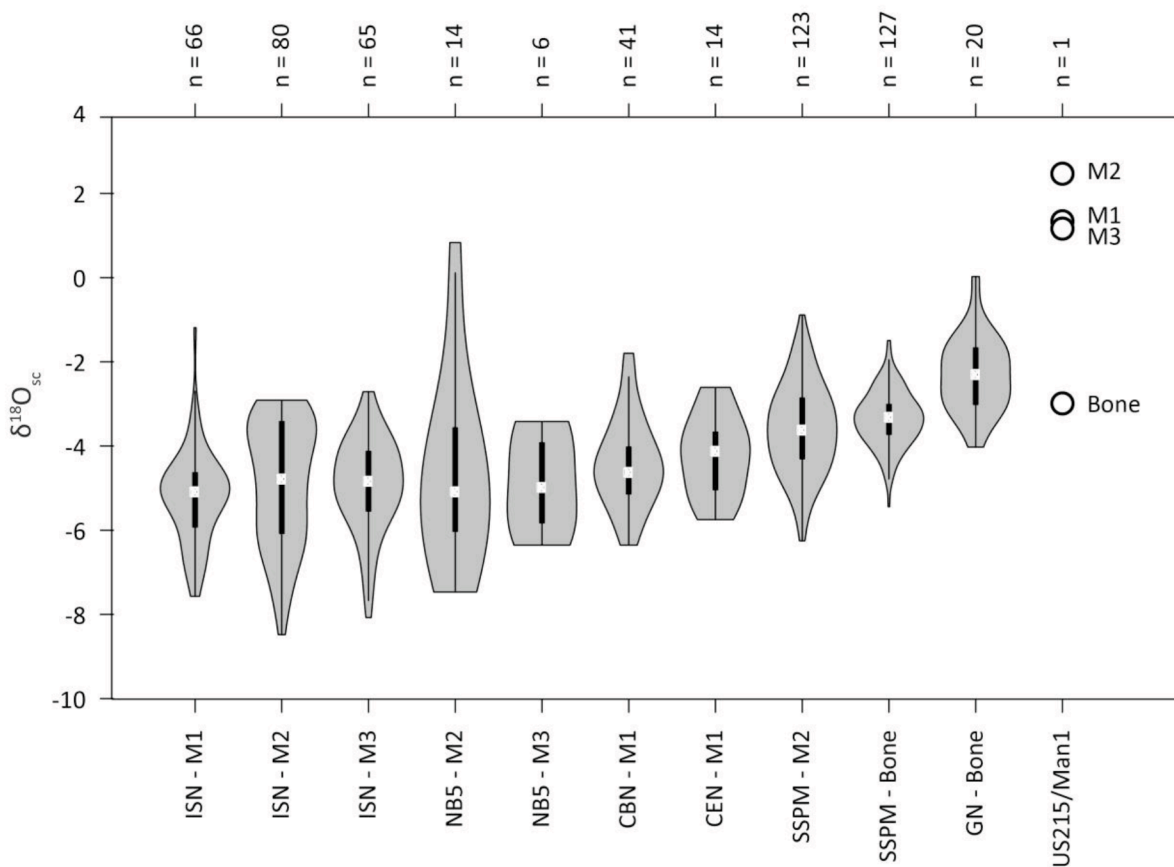


**Fig. 6.** Inter-site comparison of the  $\delta^{18}\text{O}_{\text{sc}}$  values measured on human dental samples from the Rome's region. Note: 'M1', 'M2' and 'M3' stands for permanent molars 1, 2 and 3, respectively. 'ISN' refers to Isola Sacra Necropolis, 'NB5' to Navalia Building 5, 'CBN' to Casal Bertone Necropolis, 'CEN' to Castellaccio Europarco Necropolis, 'GN' to Gabii Necropolis, and 'SSPM' to Saints Peter and Marcellinus catacombs. Bibliographic references: Prowse (2001), Prowse et al. (2007), Salesses (2015), Killgrove and Montgomery (2016), Stark (2017), Killgrove and Tykot (2018), O'Connell et al. (2019). The violins show the probability density of the data at different values, smoothed by a kernel density estimator. The boxes depict groups of data through their quartiles.

Both would be in turn balanced by the  $\delta^{18}\text{O}$  values of raw food and unprocessed drinking liquids (Brettell et al., 2012; Royer et al., 2017). The final influence on the  $\delta^{18}\text{O}_{\text{sc}}$  values, even in the hypothesis of a cumulative effect, would be therefore well below the discrepancy observed between US215/Mand1 M1 and the mean value of SSPM population M2s. Besides, culinary practices of Romans were assuredly diverse (André, 2009; Hilgers, 1969), and a mix of isotopic shifts in processed food and beverages would be expected, which would necessarily reduce the effect of the most extreme offsets induced by certain cooking methods. Furthermore, dietary habits are culturally mediated behaviors. Thus, the latter should be shared by not only one individual but the entire group, which is clearly not the case in the SSPM catacombs.

A different origin from the rest of the SSPM population appears therefore the most plausible explanation for the atypical  $\delta^{18}\text{O}_{\text{sc}}$  (enamel) values of US215/Mand1. Such high  $\delta^{18}\text{O}$  values would indicate that this individual is originated from a region characterized by a much warmer, drier climate than Lazio. US215/Mand1 seems, however, to have moved around this region during their early life. While M1 and M3 have similar  $\delta^{18}\text{O}_{\text{sc}}$  (enamel) values, they both differ from M2 by about 1‰. This difference suggests that US215/Mand1 either experienced a circular migration (between two different locations) or had a complex migration trajectory (with several changes of residences) during their childhood/adolescence in the above-described region. With a  $\delta^{18}\text{O}_{\text{sc}}$  (bone) value falling within one standard deviation from the population mean value, US215/Mand1 would have, however, inhabited several years in Rome to record the local  $\delta^{18}\text{O}$  signature in bone (Fig. 4). Furthermore, this result allows us to assign an age to this individual, which was unknown so far.

Based on the differences of  $\delta^{18}\text{O}_{\text{sc}}$  values between teeth and bone, and taking into account the rhythms of bone turnover, it can be established that US215/Mand1 was an adult. It can also be concluded that US215/Mand1 spent their life in a geological zone similar to the area of Rome, or at least a region with analogous  $^{87}\text{Sr}/^{86}\text{Sr}$  ratios to the region of Rome, during the formation of the three molars.

US215/Mand1 presents  $\delta^{13}\text{C}_{\text{sc}}$  (enamel) values of  $-12.9\%$ ,  $-12.5\%$  and  $-12.3\%$  for M1, M2 and M3, respectively (Table 3). Their mandible bone sample exhibits  $\delta^{13}\text{C}_{\text{col}}$ ,  $\delta^{15}\text{N}_{\text{col}}$ ,  $\delta^{34}\text{S}_{\text{col}}$ , and  $\delta^{13}\text{C}_{\text{sc}}$  (bone) values of  $-19.0\%$ ,  $+12.5\%$ ,  $+8.4\%$ , and  $-13.9\%$ , respectively (Table 3; Figs. 7 and 8). Taking into account the average carbon offsets between a consumer's tissues and diet (Bocherens and Drucker, 2003; Fernandes et al., 2012; Howland et al., 2003; Passey et al., 2005; Salesses, 2015; Warinner and Tuross, 2009), a  $\delta^{13}\text{C}_{\text{diet}}$  value of about  $-26/-24\%$  can be estimated.

The estimated  $\delta^{13}\text{C}_{\text{diet}}$  value is close to the mean  $\delta^{13}\text{C}_{\text{C3}}$  plants value, suggesting that US215 had a diet predominantly based on  $\text{C}_3$  terrestrial plant and herbivorous animal resources. In addition, the  $\delta^{15}\text{N}_{\text{col}}$  value (Fig. 7) is higher than the upper end of the common range for  $\text{C}_3$  terrestrial consumers (Bocherens and Drucker, 2003; Chisholm et al., 1982; Hedges and Reynard, 2007; Schoeninger et al., 1983), indicating the inclusion of organisms with relatively high trophic levels, such as aquatic resources (Craig et al., 2010; Drucker et al., 2005; Richards et al., 2015). With a  $\delta^{34}\text{S}_{\text{col}}$  value falling into the range for terrestrial/freshwater consumers (Fig. 7) (Nehlich, 2015; Peterson et al., 1985; Tsutaya et al., 2019), a consumption of marine food sources can be discarded. Freshwater fish was most likely the aquatic resource served at US215/Mand1's table. Thus, a mixed diet relying on the triad  $\text{C}_3$  plants/

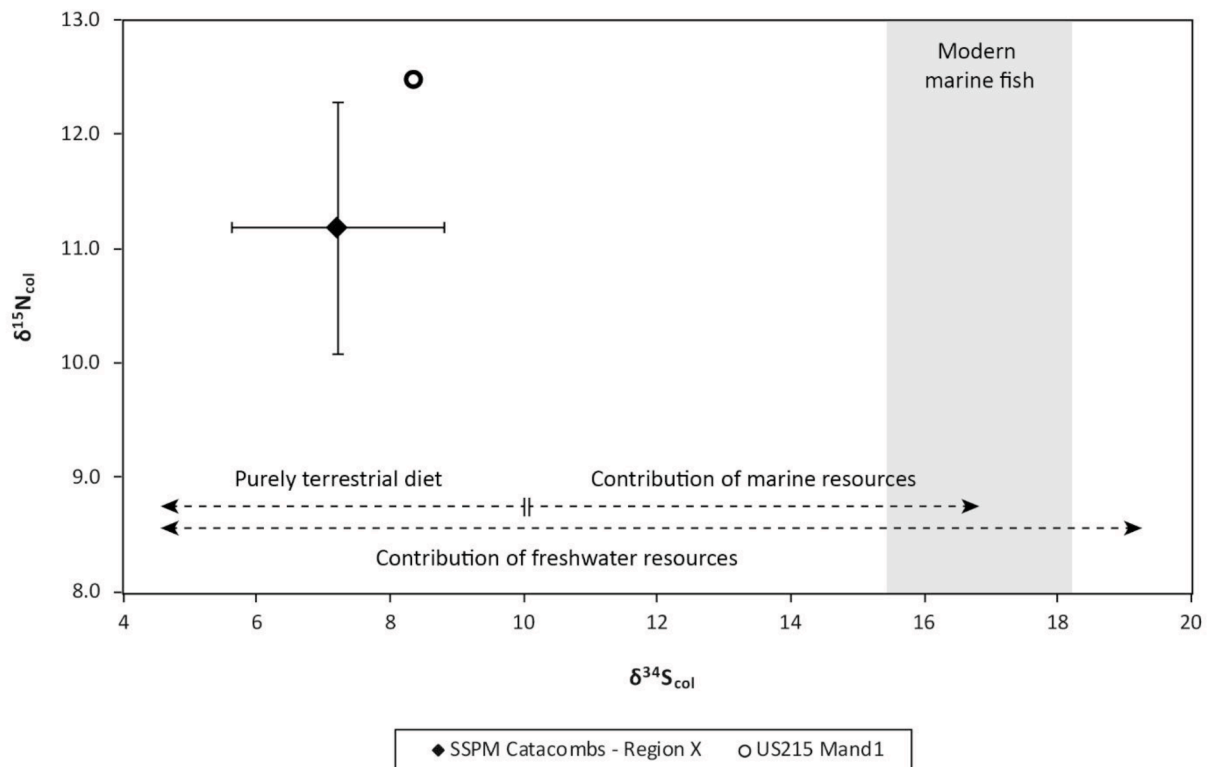


**Fig. 7.** Biplot of the  $\delta^{34}\text{S}_{\text{col}}$  and  $\delta^{15}\text{N}_{\text{col}}$  values measured on bone samples from the SSPM individuals. Note: The shaded area corresponds to the range of  $\delta^{34}\text{S}_{\text{col}}$  values for modern marine fish. The arrows indicate where individuals should stand according to their diet.

$\text{C}_3$  herbivore meat/freshwater fish products was consumed by this individual.

The US215/Mand1's dietary pattern is shared by a small batch of individuals from the Region X of the SSPM catacombs (Salesse, 2015) but also by individuals from at least two other contemporaneous populations from Rome [Catacombs of St. Callixtus (Rutgers et al., 2009); Tenuta des Duca (O'Connell et al., 2019)] (Fig. 8). Moreover, if aquatic resources are considered regardless the environment from which they originate, fish consumers are commonly identified in the Roman populations from Lazio. Diets based on aquatic resources (only marine, both freshwater and marine, or without differentiation) have been proposed as an explanation for individuals presenting high  $\delta^{15}\text{N}_{\text{col}}$  values at Castellaccio Europarco and Casal Bertone (Killgrove and Tykot, 2013), Gabii (Killgrove and Tykot, 2018), Casale del Dolce and Osteria della Fontana (Nitsch, 2012), and SSPM catacombs (Nitsch, 2012; Salesse, 2015), Isola Sacra and ANAS (Prowse et al., 2004), and finally Lucus Feroniae (Tafari et al., 2018) (Fig. 8). With a  $\delta^{15}\text{N}_{\text{col}}$  value of 12.5‰, US215/Mand1 stands among the top 10% of individuals with the most elevated  $\delta^{15}\text{N}_{\text{col}}$  values in Lazio ( $n_{10\%} = 60$ ;  $n_{\text{total}} = 603$ ) (Fig. 8). Apart a possible consumption of aquatic resources, the individuals from this top 10% group are characterized by high protein intakes. Aquatic resources, referring to fish in particular, contain generally more proteins than terrestrial animal source food (FAO, 1989; Heinz and Heutzinger, 2007; Moharrery, 2007). A consumer of aquatic products, such as US215/Mand1, has therefore a protein-rich diet.

Based on these findings, a dietary scenario including  $\text{C}_3$  plants,  $\text{C}_3$  terrestrial domesticated herbivores and freshwater fish was tested through Bayesian modelling. The Bayesian approach suggests that US215/Mand1 would have consumed  $63 \pm 13\%$  of terrestrial plant cereals,  $18 \pm 12\%$  of meat of terrestrial animals, and  $19 \pm 9\%$  of meat of freshwater fish. It estimates also that their diet would have been composed of about 28% of proteins and 72% of carbohydrates/fats. However, due to a limited baseline, this diet reconstruction must be considered as a tentative explanation, providing orders of magnitude.

Nevertheless, the Bayesian mixing model highlights that US215/Mand1 consumed terrestrial meat and aquatic resources in similar proportions and had a high protein intake.

### 5.2. Inferring the ancestry and origin of US215/Mand1 through dental morphology

The full list of recorded traits was analyzed for inter-trait correlation using Kendall tau-b, which led to the exclusion of the C1-C2 crest and the mandibular pit tubercle on the second lower molar ( $r = 1.00$ ,  $n = 8$ , no p-value was generated). The entoconulid, metaconulid and distal fossa prevalence rates exhibited no variation within the sample (0% present). An intra-observer error test by the data collector ( $r = 0.978$ ,  $p < 0.001$ ,  $n = 216$ ) has shown good agreement between observation events (Maaranen et al., 2019).

The analysis was performed on the SSPM individuals (Table 1) using 11 traits, retained after the inter-trait correlation test (Table 2). Though some of traits can be recorded in a scale, they were treated as binary if present only in grade 1 (e.g. the protostylid, presented only as a buccal pit described by Scott and Irish, 2017). Lower third molar absence, torsomolar angle and crenulation were only present in one individual per trait, so they were treated as asymmetric binary variables. How traits were treated is included in Table 1 and the full data and distance matrix in Tables C1 and C2.

A two-dimensional NMDS plot was created (Fig. 9). US215/Mand1 and US216/Mand2 resided far from the centroid, the former falling beyond the 90% confidence level and the latter even beyond 95%. Factor analysis indicated that most of the variation was contributed to enamel extension, anterior fovea, hypocone size, crenulation and deflecting wrinkle (altogether circa 60%). A hierarchical cluster analysis using complete-linkages also suggests the two individuals cluster away from the others (Fig. 10).

To explore the data further from a morphological perspective, the data was divided into clusters using the function pam from the R

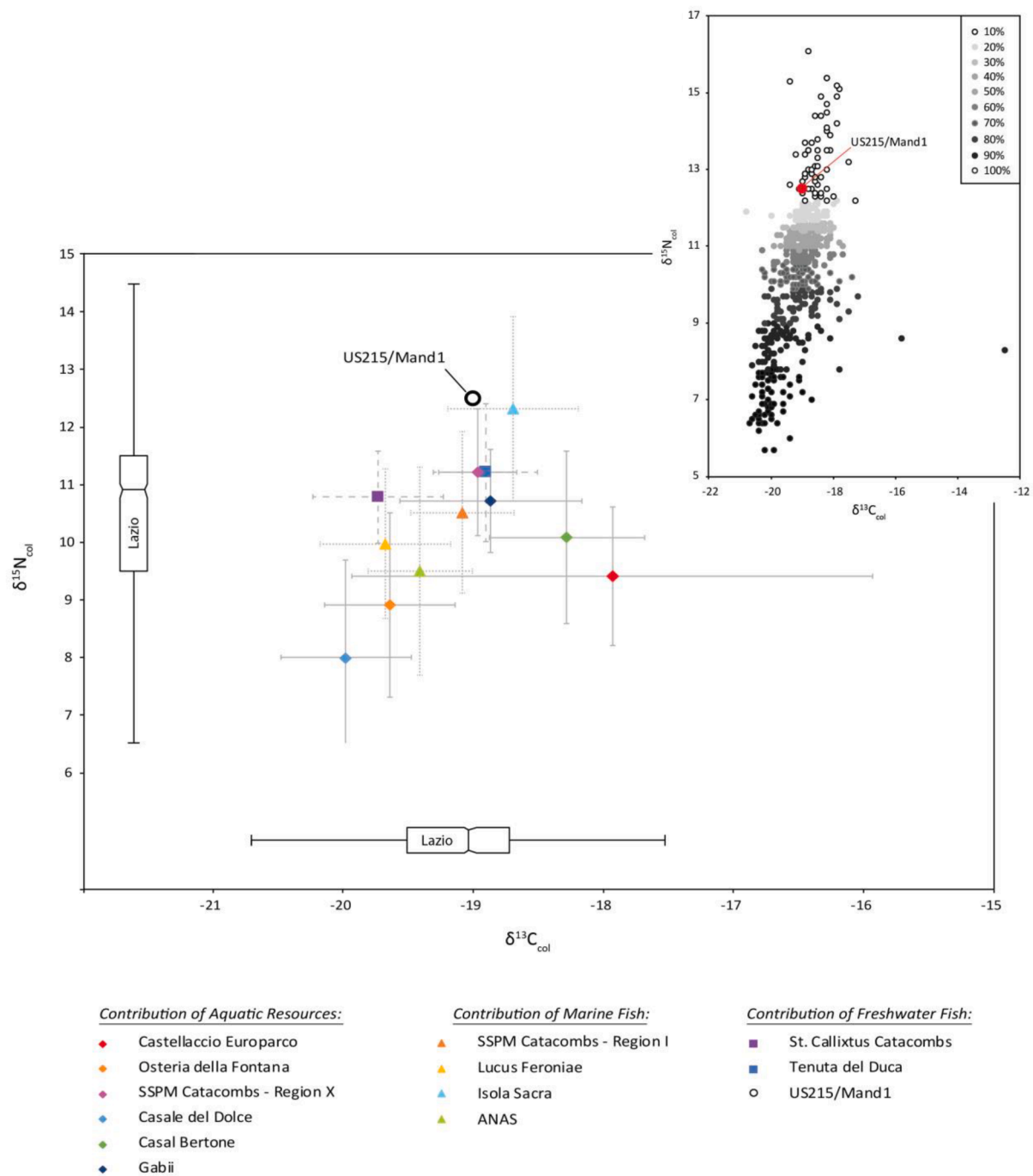


**Fig. 8.** Biplots of the  $\delta^{13}C_{col}$  and  $\delta^{15}N_{col}$  values (mean  $\pm$  1 SD) measured on human bone samples from Lazio. Note: The classification of the populations is based on the interpretations proposed by Prowse et al. (2004), Rutgers et al. (2009), Nitsch (2012), Killgrove and Tykot (2013, 2018), Salesses (2015), Tafuri et al. (2018), O’Connell et al. (2019). The boxes show the regional variability of the isotopic values. Color gradient of the scatter plot in the top right corner is based on the  $\delta^{15}N_{col}$  values.

package cluster. Silhouette method indicated an optimal number of 5 clusters (Fig. C1). The clusters were used as group indicators in the second visualization technique, t-SNE (Fig. C2), indicating that US215/Mand1 and US216/Mand2 formed their own morphological groups. The data suggest that there is heterogeneity in the SSPM dataset, with US215/Mand1 and US216/Mand2 even more morphologically different from the other individuals. Hierarchical clustering places the two individuals close to one another, but the cluster analysis divides them even from each other. It is pertinent to remember that the results are tentative, given the analysis was conducted using three molars and altogether

11 variables (Table 2). Crenulation was observed on the lower molars of US215/Mand1 but none of the other individuals in the SSPM sample.

Only five individuals from the SSPM catacombs were appropriate for the geometric morphometric outline analysis (Fig. 11). Analysis on the molar outline did not produce clustering (Fig. 11) which is probably due to small sample size. PC1 and PC2 explain 52% and 28% of the variation (cumulative 80%). Again, individuals US215/Mand1 and US216/Mand2 are separate but not significantly (ANOVA effect size;  $Z = 0.17$ ,  $p = 0.46$ ), unsurprising given the distance between the individuals along PC1. Most of the variation in the shape was captured in the lower third

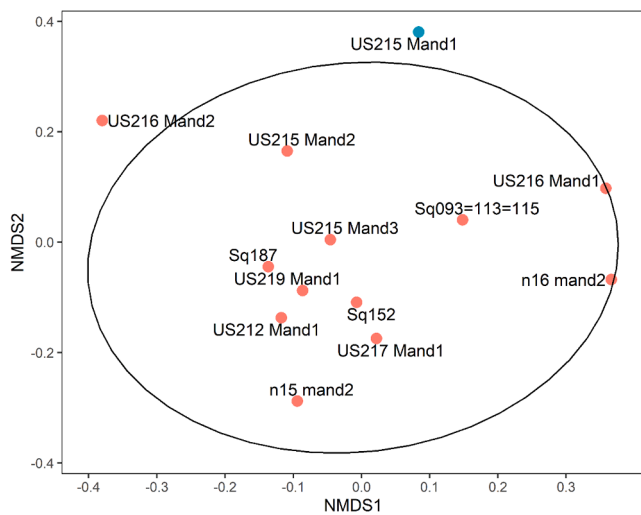


**Fig. 9.** NMDS plot was created from the distance matrix (see Table C2) of the SSPM individuals. The ellipse marks the 90% confidence level for the sample. Both US215 Mand1 and US216 Mand2 fall far away from the rest of the individuals.

molar (Fig. C3), the most variable tooth in the dentition. The inherent variation of this tooth could explain why each configuration was so different, which coupled with the small sample size could not generate meaningful clusters.

### 5.3. aDNA, an attempt to address the provenance of US215/Mand1

No Y-chromosome SNPs could be characterized for any of the targeted samples, and very rare mitochondrial SNPs were obtained (Supplementary File D). Mitochondrial results were conclusive only for the sample US219/Mand1 from the chamber X83 to which replicable haplogroup H1 could be assigned (Supplementary File C). The latter cannot be, however, specified with the type of investigation applied here. Haplogroup H is the most common in today's Europe, and for example reach 38.99% in Italy (Turchi et al., 2008). As the current repartition of the sub-haplogroup H1 covers Europe as well as North Africa (Gleize et al., 2016), it cannot give a more precise information for the origin of individual US219/Mand1, who could come from Italy as well as from other European or North African regions. The other mitochondrial results were either non-replicable (Sq108 from X83), or inconsistent

(US215/Mand1 from X83), or too scarce (n°13/Mand1 from X81; Sq152 and US219/Mand2 from X83) (Supplementary File C). The aDNA analyses clearly demonstrated a major DNA degradation in the specific case of these individuals, which could easily be explained by the environmental conditions inside the SSPM catacombs combined to specific funerary treatments (presence of lime) highly detrimental to DNA preservation.

## 6 Discussion

If regional-scale predictive  $^{87}\text{Sr}/^{86}\text{Sr}$  maps for southern Europe, Near East and North Africa are still missing, global and regional  $\delta^{18}\text{O}$  isoscapes are available for the areas covered by the Roman Empire at its greatest extent (i.e. during the 2nd century CE). Based on the OIPC maps ([http://wateriso.utah.edu/waterisotopes/pages/data\\_access/figures.html](http://wateriso.utah.edu/waterisotopes/pages/data_access/figures.html)), three locations inside or in the immediate vicinity of the Roman Empire can be identified as potential regions of origin for US215/Mand1: the Arabian Peninsula, the Nile Valley and within the central Sahara Desert.

Measurements on modern rivers waters but also on archaeological human and faunal remains sampled in these three regions corroborate the predictive  $\delta^{18}\text{O}$  models. Upstream at Khartoum, Farah et al. (2000) and Iacumin et al. (2016) determined mean  $\delta^{18}\text{O}_{\text{water}}$  values for the main Nile of +2.5‰ and +1.8‰, respectively. Similarly, downstream at Cairo, Buzon and Bowen (2010) reported a mean  $\delta^{18}\text{O}_{\text{water}}$  value for the Nile River of +2.3‰. In a synthesis effort, Dufour et al. (2018) showed that the  $\delta^{18}\text{O}_{\text{water}}$  values could, however, vary a bit all along the river. Nevertheless, the  $\delta^{18}\text{O}_{\text{water}}$  values for the Nile would have remained broadly stable from the Late Period of ancient Egypt/the Meroitic Period in Sudan to nowadays (Touzeau et al., 2013). This is mainly supported by the high and positive  $\delta^{18}\text{O}$  values displayed by human and animal samples during that time span (Buzon et al., 2019; Iacumin et al., 1996, 2016; Touzeau et al., 2013). Also, oxygen isotope compositions of tooth enamel from archaeological faunal specimens collected in the Libyan Sahara are in good accordance with the  $\delta^{18}\text{O}$  values of modern precipitations (di Lernia et al., 2013). Besides, the variations of  $\delta^{18}\text{O}_{\text{Sc}}$  (enamel) values suggest that US215/Mand1 spent their early life to change of residences in one of these three regions.

From a dental morphological perspective, US215/Mand1 differs from the rest of the SSPM population (Figs. 9–11 and C2). Furthermore, the unique presence and high expression (grades  $\geq 1$  for M1 and M2; grade = 2 for M3) of crenulations on the US215/Mand1's molars are of particular interest as they could be informative of a specific population

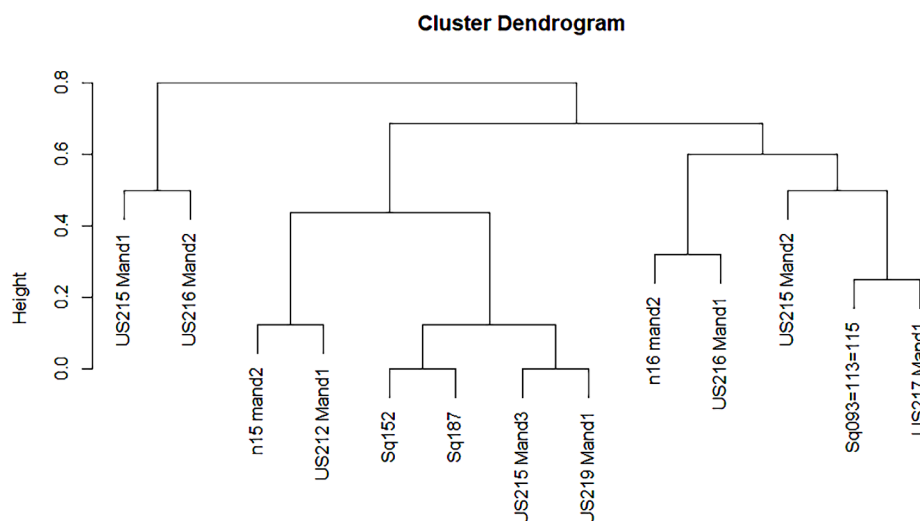


**Fig. 10.** Hierarchical dendrogram generated from the SSPM non-metric dental dataset. Note: The agglomerative method complete linkage was used. US215/Mand1 (ID 206) and US216/Mand2 (ID 210) are separated from the rest.

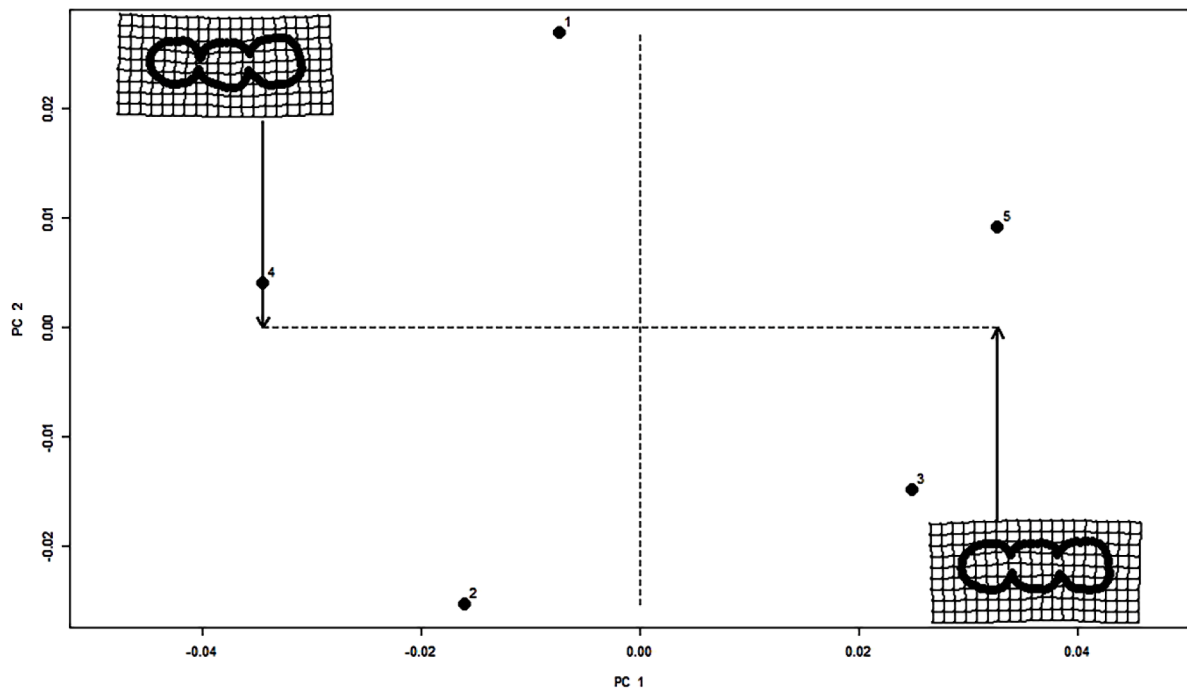


Fig. 11. PCA plot performed on the geometric morphometric data obtained on the SSPM individuals. Note: PC1 explains 52% of the shape variation, and PC2 28%. ID1 = X81\_n°14/Mand2, ID2 = X83\_US215/Mand1, ID3 = X83\_US216/Mand2, ID4 = X83\_US217/Mand1, and ID5 = X83\_US219/Mand1.

history. This dental nonmetric trait has notably been identified as being more common among African and African-derived populations (Pilloud et al., 2018; Rhine, 1990). Especially, Pilloud and colleagues (2018) established that there was a relationship between the presence of grades equal to or greater than 1 and the modern American Black and South African samples they studied. Therefore, the complex molar surfaces as well as the molar crenulation trait presence would support an African ancestry of US215/Mand1.

After excluding outliers (Grubb's tests), the  $^{87}\text{Sr}/^{86}\text{Sr}$  ratios display by humans vary from 0.70731 to 0.70807 in Egypt, from 0.70658 to 0.70912 in Sudan, and from 0.70975 to 0.71293 in central Sahara Desert (Fig. 12) (Tafari et al. 2006; Buzon et al., 2007; Sereno et al., 2008; Buzon and Simonetti, 2013; di Lernia and Tafari, 2013; di Lernia et al., 2013; Stojanowski and Knudson, 2014; Schrader et al., 2019). Based on these data, neither the northern part of the Nile Valley nor the Saharan area appear to be places from where US215/Mand1 could originate. Moreover, if at first glance the Third Cataract region could be a possible origin for US215/Mand1 (core  $^{87}\text{Sr}/^{86}\text{Sr}$  range = 0.70696–0.70912; Fig. 12), Buzon and colleagues have suggested that individuals with  $^{87}\text{Sr}/^{86}\text{Sr}$  values greater than 0.70783 did not belong to this locality but were migrants from northern lands (Buzon and Simonetti, 2013; Buzon et al., 2016). Among the latter stands the Second Cataract region. Because of its geological complexity, this region presents a large local  $^{87}\text{Sr}/^{86}\text{Sr}$  range, varying between 0.704 and 0.717 (Schrader et al., 2019). Animal samples recovered near the Second Cataract exhibit a wide distribution of their  $^{87}\text{Sr}/^{86}\text{Sr}$  values as well, ranging between 0.70667 and 0.70933 (after removing outliers via Grubb's test) (Fig. 12). This represents a pertinent area where US215/Mand1 could have spent their early life. Additionally, cattle from Nubian sites show generally a broad range of  $^{87}\text{Sr}/^{86}\text{Sr}$  values (Fig. 12), which suggests that imports and/or transhumance of some animals may have occurred (Buzon and Simonetti, 2013; Schrader et al., 2019). Non-local cattle were most probably brought from surrounding regions as tributes or traded with communities – either nomadic or not – from the arid desert edge (Buzon and Simonetti, 2013; Iacumin et al., 2001; Thompson et al., 2008). Thus, cattle Sr variability would indicate that various – unknown – localities from Sudan could have been possible places of origin for

US215/Mand1. Even though available  $^{87}\text{Sr}/^{86}\text{Sr}$  values for humans from central Sahara Desert do not fit with those of US215/Mand1, one could be intrigued by the isotopic composition of an equid specimen recovered in the Messak Mountains (di Lernia et al., 2013). Of the two measurements taken along its M3 crown, one is similar to the  $^{87}\text{Sr}/^{86}\text{Sr}$  values exhibited by US215/Mand1 ( $^{87}\text{Sr}/^{86}\text{Sr}_{\text{MK07/39C1-09}} = 0.7087$  in di Lernia et al., 2013) (Fig. 12). If this animal moved in that region, it also suggests that the central Sahara Desert cannot be excluded as a potential origin of US215/Mand1.

Together these lines of evidence converge and argue for an origin beyond the African Roman frontier for US215/Mand1, making this individual the first example of an African-born migrant revealed by a multi-analytical approach including isotopic analysis and discovered in the Imperial capital. Moreover, US215/Mand1 has experienced the second longest migration across the Roman Empire highlighted by direct evidence, after the one discovered in Roman York (UK) discussed by Martiniano et al. (2016) who suggested a Middle Eastern origin based on genomic and isotope data.

Fish, whether marine or freshwater, was a social marker at the time of the imperial era (André, 2009). While there are many indications that rich and poor alike had access to resources of the same nature, they did have different dietary practices (André, 2009; Garnsey and Saller, 1987; Schirmer, 2014; Spurr, 1983). The quality but also the diversity of the food consumed, as well as the way it was prepared, varied considerably between the low and high strata of Roman society (André, 2009; Purcell, 1995; Schirmer, 2014). Freshwater fish, in Rome as in other parts of the Empire, was consumed in large quantities only by the most humble or ordinary people (André, 2009; Marzano, 2018). The wealthier individuals and elites would occasionally consume it, but undoubtedly preferred marine fish. In addition to their taste, marine fish also represented a potent sign of wealth. In short, fish, whether marine or freshwater, was a social marker at the time of the imperial era (see André, 2009; Marzano, 2018 for thorough historical syntheses). Based on the isotopic results showing US215/Mand1 consuming freshwater fish in a significant proportion, one can suggest that US215/Mand1 had probably a modest socio-economic status and belonged to the low strata of the Roman society.

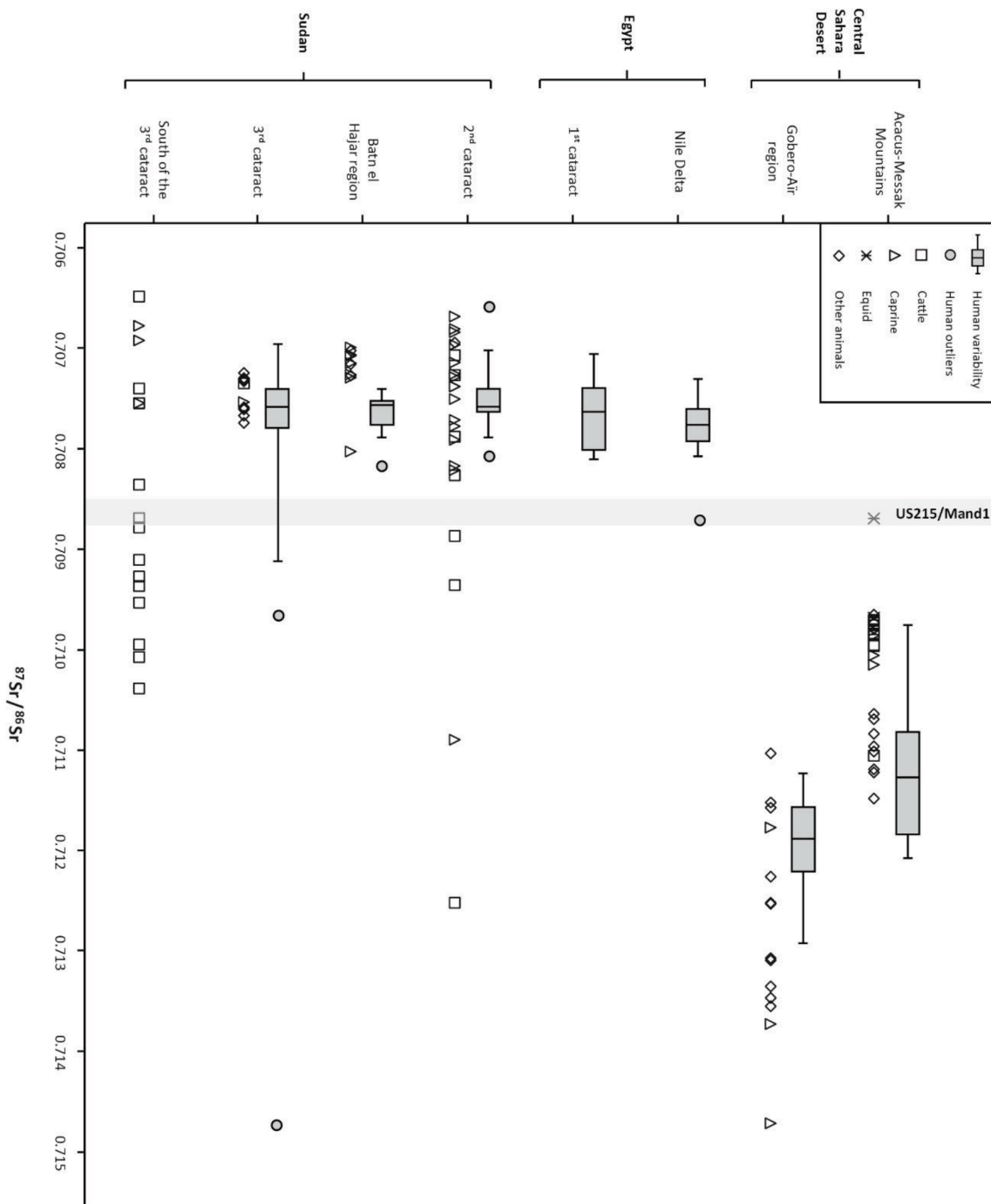


**Fig. 12.** Variability of the  $^{87}\text{Sr}/^{86}\text{Sr}$  ratios measured on human and faunal remains from North African region. Bibliographic references: Tafuri et al. (2006), Sereno et al. (2008), di Lernia and Tafuri (2013), di Lernia et al. (2013), Stojanowski and Knudson (2014) for Central Sahara Desert; Buzon et al. (2007), Buzon and Simonetti (2013), Schrader et al. (2019) for Egypt-Sudan. Note: Populations dates from different times periods. Boxes represent the range of variation of human values. Outliers have been identified through Grubb's tests. The shaded area corresponds to the range of  $^{87}\text{Sr}/^{86}\text{Sr}$  values exhibit by the molars of US215/Mand1.

These different lines of evidence support two storylines for US215/Mand1. The least likely would be that US215/Mand1 was a free man or woman originated from the northern part of the African continent, who would have settled in the city of Rome for specific business. The most likely would be that after spending their early life moving in the vicinity of the Nile Valley or within the central Sahara Desert, possibly due to a nomadic condition or a peregrine status, US215/Mand1 could have experienced forced migration as a slave and was eventually shipped to Rome along trade routes. On the basis of the evidence we have, it is unfortunately impossible to assess whether US215/Mand1 belonged to a

private household or was owned by Rome's people, acting as a public slave. More broadly, the presence of US215/Mand1 in the mass graves of the SSPM catacombs provides a better understanding of the epidemic. As it seems that individuals from all strata of Rome were buried together in these sepulchral spaces, the epidemic was not selective from a socio-economic point of view. This would confirm the snapshot and the uncommon nature of this archaeological context.

## 7 Conclusion

Based on a multi-tissue sampling strategy including molar teeth and mandibular cortical bone, our multi-analytical approach using isotopic ( $\delta^{13}\text{C}$ ,  $\delta^{15}\text{N}$ ,  $\delta^{18}\text{O}$ ,  $\delta^{34}\text{S}$ ,  $^{87}\text{Sr}/^{86}\text{Sr}$ ), dental morphology (geometric morphometrics, nonmetric traits) and ancient DNA (mitochondrial DNA, Y chromosome) analyses has refined the origin and life history of US215/Mand1 buried in the X83 mass grave from the SSPM catacombs. Obtained lines of evidence suggest that this individual was born beyond the southern *limes*, possibly in the vicinity of the Nile Valley or within the central Sahara Desert, and experienced diachronic changes of residence during their early life, conceivably due to a nomadic condition or a peregrine status. The way US215/Mand1 arrived in the imperial capital is still hypothetical, although it seems likely that he/she could have undergone forced migration and eventually transported as a slave to Rome. It cannot be totally excluded, however, that US215/Mand1 was a free man or woman originated from North Africa, settling in the city of Rome for specific business affairs. This study presents direct evidence of one of the unique cases of long-distance migration across the Empire of a non-Roman. In particular, it highlights for the first time the journey of a North African-born individual who died in the Eternal city. Enslaved or not, US215/Mand1 clearly illustrates and confirms the cosmopolitan character of Rome. Finally, this study restates the importance and usefulness of multi-proxy investigations for reconstructing the identities of past human individuals recovered in archaeological contexts.

## Declaration of Competing Interest

The authors declare that they have no known competing financial interests or personal relationships that could have appeared to influence the work reported in this paper.

## Acknowledgments

The main author wishes to express his gratitude to R. Giuliani, chief inspector of the Vatican's Pontificia Commissione di Archeologia Sacra for the material authorization. The main author thanks J. Ughetto-Monfrin (SSMIM, France), C. Wurster (James Cook University, Australia) and J. Wilson (University of South Florida, USA) for their support with the stable isotope analysis. The main author acknowledges C. Snoeck (Vrije Universiteit Brussel, Belgium) and M. Vercauteren (Université Libre de Bruxelles, Belgium) for useful discussions. Finally, all the authors are grateful to the editors and reviewers for their time and constructive comments on our manuscript.

## Funding

Financial support for this research was provided by the Aquitaine Region (France) and the Maison des Sciences de l'Homme d'Aquitaine (Pessac, France) through the project "L'église, les vivants, les morts" directed by D. Castex, and the Action Thématique du MNHN "Biominingalization" (Paris, France) led by E. Dufour for research support. Postdoctoral fellowships were granted to K. Salessé through the project "Quantifying the Roman diet" funded by the Shohet Scholars Grant Program of the International Catacomb Society (Boston, USA) directed by R. H. Tykot and K. Salessé, and the CRUMBEL project ("CREmations, Urns and Mobility: ancient population dynamics in BELgium"), funded by Fonds Wetenschappelijk Onderzoek – Vlaanderen (FWO) and the Fonds de la Recherche Scientifique (F.R.S.-FNRS) within the framework of the Excellence of Science (EOS) program (n°30999782) in Belgium, directed by M. Vercauteren, C. Snoeck, D. Tys, G. De Mulder and M. Boudin.

## Appendix A. Supplementary data

Supplementary data to this article can be found online at <https://doi.org/10.1016/j.jasrep.2021.103011>.

## References

- Abrecht, R.R., 2019. An immigrant neighbourhood in ancient Rome. *Urban Hist.* 1–21.
- Alvarez, H.P., 2000. Grandmother hypothesis and primate life histories. *Am. J. Phys. Anthropol.* 113, 435–450.
- Ambrose, S.H., 1990. Preparation and characterization of bone and tooth collagen for isotopic analysis. *J. Archaeol. Sci.* 17, 431–451.
- André, J., 2009. *L'alimentation et la cuisine à Rome*. Les Belles Lettres, Paris.
- Balasse, M., Ambrose, S.H., Smith, A.B., Price, T.D., 2002. The seasonal mobility model for prehistoric herders in the south-western Cape of South Africa assessed by isotopic analysis of sheep tooth enamel. *J. Archaeol. Sci.* 29, 917–932.
- Balter, V., Lécuyer, C., 2010. Determination of Sr and Ba partition coefficients between apatite from fish (*Sparus aurata*) and seawater: the influence of temperature. *Geochim. Cosmochim.* 74, 3449–3458.
- Blanchard, P., Coquerelle, M., Giuliani, R., Ricciardi, M., 2007. A mass grave from the catacomb of Saints Peter and Marcellinus in Rome, second-third century AD. *Antiquity* 81, 989–998.
- Blanchard, P., Réveillas, H., Kacki, S., Castex, D., 2015. La catacombe des Saints Pierre-et-Marcellin à Rome (I<sup>er</sup>-III<sup>e</sup> s.) : discussion sur l'origine des défunts et leur décès. In: Branco, G., Rocha, L., Duarte, C., de Oliveira, J., Ramirez, B. (Eds.), *Arqueologia de Transição: O Mundo Funerário*. Actas do II Congresso Internacional Sobre Arqueologia de Transição (29 de Abril a 1 de Maio 2013). CHAIA, Évora, pp. 197–216.
- Bocherens, H., Drucker, D., 2003. Trophic level isotopic enrichment of carbon and nitrogen in bone collagen: case studies from recent and ancient terrestrial ecosystems. *Int. J. Osteoarchaeol.* 13 (1), 46–53.
- Bocherens, H., Drucker, D.G., Taubald, H., 2011. Preservation of bone collagen sulphur isotopic compositions in an early Holocene river-bank archaeological site. *Palaeogeogr. Palaeoclimatol. Palaeoecol.* 310, 32–38.
- Bocherens, H., Fizez, M., Cuif, J.P., Jaeger, J.-J., Michard, J.-G., Mariotti, A., 1988. Premières mesures d'abondances isotopiques naturelles en  $^{13}\text{C}$  et en  $^{15}\text{N}$  de la matière organique fossile de dinosaure. Application à l'étude du régime alimentaire du genre *Anatosaurus* (*Ornithischia*, *Hadrosauridae*). *C. R. l'Acad. Sci.* 306, 1521–1526.
- Bocherens, H., Fizez, M., Mariotti, A., Lange-Badre, B., Vandermeersch, B., Borel, J.P., Bellon, G., 1991. Isotopic biogeochemistry ( $^{13}\text{C}$ ,  $^{15}\text{N}$ ) of fossil vertebrate collagen: application to the study of a past food web including Neandertal man. *J. Hum. Evol.* 20, 481–492.
- Bookstein, F.L., 1997. Landmark methods for forms without landmarks: morphometrics of group differences in outline shape. *Med. Image Anal.* 1, 225–243.
- Brettell, R., Montgomery, J., Evans, J., 2012. Brewing and stewing: the effect of culturally mediated behaviour on the oxygen isotope composition of ingested fluids and the implications for human provenance studies. *J. Anal. At. Spectrom.* 27, 778–785.
- Britton, K., Fuller, B.T., Tütken, T., Mays, S., Richards, M.P., 2015. Oxygen isotope analysis of human bone phosphate evidences weaning age in archaeological populations. *Am. J. Phys. Anthropol.* 157, 226–241.
- Buzon, M.R., Bowen, G.J., 2010. Oxygen and carbon isotope analysis of human tooth enamel from the New Kingdom site of Tombos in Nubia. *Archaeometry* 52, 855–868.
- Buzon, M.R., Simonetti, A., Creaser, R.A., 2007. Migration in the Nile Valley during the New Kingdom period: A preliminary strontium isotope study. *J. Archaeol. Sci.* 34 (9), 1391–1401.
- Buzon, M.R., Schrader, S.A., Bowen, G.J., 2019. Isotopic approaches to mobility in northern Africa: a bioarchaeological examination of Egyptian/Nubian interaction in the Nile Valley. In: Mattingly, D.J., Sterry, M., Gatto, M.C., Ray, N. (Eds.), *Burials, Migration and Identity in the Ancient Sahara and Beyond*. Cambridge University Press, Cambridge, pp. 223–246.
- Buzon, M.R., Simonetti, A., 2013. Strontium isotope ( $^{87}\text{Sr}/^{86}\text{Sr}$ ) variability in the Nile Valley: identifying residential mobility during ancient Egyptian and Nubian sociopolitical changes in the New Kingdom and Napatan periods. *Am. J. Phys. Anthropol.* 151, 1–9.
- Buzon, M.R., Smith, S.T., Simonetti, A., 2016. Entanglement and the formation of the ancient Nubian Napatan state. *Am. Anthropol.* 118, 284–300.
- Castex, D., Blanchard, A., 2011. Témoignages archéologiques de crise(s) épidémique(s): la catacombe des Saints Marcellin et Pierre (Rome, fin I<sup>er</sup>-III<sup>e</sup> s.). In: Castex, D., Courtaud, P., Duday, H., Le Mort, F., Tillier, A.-M. (Eds.), *Le regroupement des morts. Genèse et diversité archéologique*. Editions Ausonius - Maison des Sciences de l'Homme d'Aquitaine, Bordeaux, pp. 281–293.
- Castex, D., Blanchard, A., Giuliani, R., Ricciardi, M., 2007. Les ensembles funéraires du secteur central de la catacombe des Saints Pierre et Marcellin (Rome, I<sup>er</sup>-III<sup>e</sup> siècle): caractérisation, hypothèses d'interprétations et perspectives de recherches. *Mélanges de l'École française de Rome. Antiquité* 119, 274–282.
- Castex, D., Blanchard, A., Réveillas, H., Kacki, S., Giuliani, R., 2009. Les sépultures du secteur central de la catacombe des Saints Pierre-et-Marcellin (Rome). Etat des analyses bio-archéologiques et perspectives. *Mélanges de l'École française de Rome. Antiquité* 121, 287–297.
- Castex, D., Blanchard, P., Kacki, S., Réveillas, H., Giuliani, R., 2011. Le secteur central de la catacombe des Sts Pierre-et-Marcellin (Rome, I<sup>er</sup>-III<sup>e</sup> siècle). *Indices*

- archéologiques d'une crise brutale de mortalité. *Mélanges de l'École Française de Rome. Chronique* 123, 274–280.
- Castex, D., Kacki, S., Reveillas, H., Souquet-Leroy, I., Sachau-Carcel, G., Blaizot, F.R., Blanchard, P., Duday, H., 2014. Revealing archaeological features linked to mortality increases. *Anthropologie* 52, 299–318.
- Chenery, C.A., Pashley, V., Lamb, A.L., Sloane, H.J., Evans, J.A., 2012. The oxygen isotope relationship between the phosphate and structural carbonate fractions of human bioapatite. *Rapid Commun. Mass Spectrom.* 26, 309–319.
- Chisholm, B.S., Nelson, D.E., Schwarcz, H.P., 1982. Stable carbon isotope ratios as a measure of marine versus terrestrial protein in ancient diets. *Science* 216, 1131–1132.
- Collyer, M.L., Adams, D.C., 2018. An R package for fitting linear models to high-dimensional data using residual randomization. *Methods Ecol. Evol.* 9, 1772–1779.
- Coplen, T.B., 1988. Normalization of oxygen and hydrogen isotope data. *Chem. Geol.: Isotope Geosc. Sect.* 72, 293–297.
- Craig, O.E., Biazio, M., Colonese, A.C., di Giuseppe, Z., Martinez-Labarga, C., lo Vetro, D., Lelli, R., Martini, F., Rickards, O., 2010. Stable isotope analysis of Late Upper Palaeolithic human and faunal remains from Grotta del Romito (Cosenza), Italy. *J. Archaeol. Sci.* 37, 2504–2512.
- Daux, V., Lécuyer, C., Héran, M.A., Amiot, R., Simon, L., Fourel, F., Martineau, F., Lynnerup, N., Reyhler, H., Escarguel, G., 2008. Oxygen isotope fractionation between human phosphate and water revisited. *J. Hum. Evol.* 55, 1138–1147.
- de Ligt, L., Tacoma, L.E., 2016. *Migration and mobility in the Early Roman Empire*. Brill, Leiden.
- De Muynck, D., Huelga-Suarez, G., Van Heghe, L., Degryse, P., Vanhaecke, F., 2009. Systematic evaluation of a strontium-specific extraction chromatographic resin for obtaining a purified Sr fraction with quantitative recovery from complex and Ca-rich matrices. *J. Anal. At. Spectrom.* 24, 1498–1510.
- DeNiro, M.J., 1985. Postmortem preservation and alteration of in vivo bone collagen ratios in relation to palaeodietary reconstruction. *Nature* 317, 806–809.
- Deviesse, T., Ribechini, E., Castex, D., Stuart, B., Regert, M., Colombini, M.P., 2017. A multi-analytical approach using FTIR, GC/MS and Py-GC/MS revealed early evidence of embalming practices in Roman catacombs. *Microchem. J.* 133, 49–59.
- di Lernia, S., Tafuri, M.A., 2013. Persistent deathplaces and mobile landmarks: The Holocene mortuary and isotopic record from Wadi Takarkori (SW Libya). *J. Anthropol. Archaeol.* 32 (1), 1–15. <https://doi.org/10.1016/j.jaa.2012.07.002>.
- di Lernia, S., Tafuri, M.A., Gallinaro, M., Alhaighe, F., Balasse, M., Cavorsi, L., Fullagar, P.D., Mercuri, A.M., Monaco, A., Perego, A., Zerboni, A., 2013. Inside the "African Cattle Complex": Animal Burials in the Holocene Central Sahara. *PLoS ONE* 8, e56879.
- Dobberstein, R.C., Collins, M.J., Craig, O.E., Taylor, G., Penkman, K.E.H., Ritz-Timme, S., 2009. Archaeological collagen: why worry about collagen diagenesis? *Archaeol. Anthropol. Sci.* 1, 31–42.
- Drucker, D., Henry-Gambier, D., Lenoir, M., 2005. Alimentation humaine au cours du Magdalénien en Gironde d'après les teneurs en isotopes stables ( $^{13}\text{C}$ ,  $^{15}\text{N}$ ) du collagène. *Paléo* 17, 57–72.
- Dupras, T.L., Schwarcz, H.P., Fairgrieve, S.I., 2001. Infant feeding and weaning practices in Roman Egypt. *Am. J. Phys. Anthropol.* 115, 204–212.
- Dufour, E., Van Neer, W., Vermeersch, P.M., Patterson, W.P., 2018. Hydroclimatic conditions and fishing practices at Late Paleolithic Makhadma 4 (Egypt) inferred from stable isotope analysis of otoliths. *Quat. Int.* 471, 190–202.
- FAO, 1989. *Yield and Nutritional Value of the Commercially more Important Fish Species*. Food and agriculture organization of the United Nations, Rome.
- Farah, E.A., Mustafa, E.M.A., Kumai, H., 2000. Sources of groundwater recharge at the confluence of the Nile, Sudan. *Environ. Geol.* 39, 667–672.
- Fernandes, R., Nadeau, M.J., Grootes, P.M., 2012. Macronutrient-based model for dietary carbon routing in bone collagen and bioapatite. *Archaeol. Anthropol. Sci.* 4, 291–301.
- Fernandes, R., Millard, A.R., Brabec, M., Nadeau, M.-J., Grootes, P., 2014. Food Reconstruction Using Isotopic Transferred Signals (FRUITS): a bayesian model for diet reconstruction. *PLoS ONE* 9, e87436.
- Garnsey, P., Saller, R.P., 1987. *The Roman Empire: Economy, Society, and Culture*. University of California Press, Berkeley.
- Garvie-Lok, S.J., 2001. In: *Loaves and Fishes: A Stable Isotope Reconstruction of Diet in Medieval Greece*. University of Calgary, Calgary, p. 525.
- George, M., 2003. Images of Black slaves in the Roman empire. *Syllecta Classica* 14, 161–185.
- Giuliani, R., Castex, D., Blanchard, P., Coquerelle, M., 2007. La scoperta di un nuovo santuario nella catacomba dei SS. Marcellino e Pietro e lo scavo antropologico degli insiemi funerari annessi. Risultati preliminari di un'indagine multidisciplinare. *Rend. Pontificia Accad. Romana Archeol.* 79, 83–124.
- Gleize, Y., Mendisco, F., Pemonge, M.-H., Hubert, C., Groppi, A., Houix, B., Deguilloux, M.-F., Breuil, J.-Y., 2016. Early medieval Muslim graves in France: first archaeological, anthropological and palaeogenomic evidence. *PLoS ONE* 11, e0148583.
- Gordon, M.L., 1924. The nationality of slaves under the early Roman empire. *J. Roman Stud.* 14, 93–111.
- Gower, J.C., 1971. A general coefficient of similarity and some of its properties. *Biometrics* 27, 857–871.
- Hedges, R.E.M., Reynard, L.M., 2007. Nitrogen isotopes and the trophic level of humans in archaeology. *J. Archaeol. Sci.* 34, 1240–1251.
- Heinz, G., Heutzinger, P., 2007. *Meat Processing Technology for Small- to Medium-scale Producers*. Food and Agriculture Organization of the United Nations, Bangkok.
- Herring, D.A., Saunders, S.R., Katzenberg, M.A., 1998. Investigating the weaning process in past populations. *Am. J. Phys. Anthropol.* 105, 425–439.
- Hilgers, W., 1969. *Lateinische gefässnamen*. Rheinland-Verlag, Düsseldorf.
- Howland, M.R., Corr, L.T., Young, S.M., Jones, V., Jim, S., van der Merwe, N.J., Mitchell, A.D., Evershed, R.P., 2003. Expression of the dietary isotope signal in the compound-specific  $\delta^{13}\text{C}$  values of pig bone lipids and amino acids. *Int. J. Osteoarchaeol.* 13, 54–65.
- Iacumin, P., Bocherens, H., Chaix, L., 2001. Keratin C and N stable isotope ratios of fossil cattle horn from Kerma (Sudan): a record of dietary changes. *Quaternario* 14, 41–46.
- Iacumin, P., Bocherens, H., Chaix, L., Mاريو, A., 1998. Stable carbon and nitrogen isotopes as dietary indicators of ancient Nubian populations (Northern Sudan). *J. Anthropol. Archaeol.* 25, 293–301.
- Iacumin, P., Bocherens, H., Mariotti, A., Longinelli, A., 1996. An isotopic palaeoenvironmental study of human skeletal remains from the Nile Valley. *Palaeogeogr. Palaeoclimatol., Palaeoecol.* 126, 15–30.
- Iacumin, P., Di Matteo, A., Usai, D., Salvatori, S., Venturilli, G., 2016. Stable isotope study on ancient populations of central Sudan: insights on their diet and environment. *Am. J. Phys. Anthropol.* 160, 498–518.
- Irish, J.D., 2005. Population continuity vs. discontinuity revisited: Dental affinities among Late Paleolithic through Christian-era Nubians. *Am. J. Phys. Anthropol.* 128, 520–535.
- Kacki, S., Réveillas, H., Sachau-Carcel, G., Giuliani, R., Blanchard, P., Castex, D., 2014. Réévaluation des arguments de simultanéité des dépôts de cadavres: l'exemple des sépultures plurielles de la catacombe des Saints Pierre-et-Marcellin (Rome). *Bull. mémoires de la Société d'anthropologie de Paris* 1–10.
- Keenleyside, A., Schwarcz, H.P., Stirling, L., Ben Lazreg, N., 2009. Stable isotopic evidence for diet in a Roman and Late Roman population from Leptiminus, Tunisia. *J. Archaeol. Sci.* 36, 51–63.
- Kendall, D.G., 1984. Shape manifolds, procrustean metrics, and complex projective spaces. *Bull. London Math. Soc.* 16, 81–121.
- Kennedy, G.E., 2005. From the ape's dilemma to the weanling's dilemma: early weaning and its evolutionary context. *J. Hum. Evol.* 48, 123–145.
- Killgrove, K., Tykot, R.H., 2013. Food for Rome: a stable isotope investigation of diet in the Imperial period (1st–3rd centuries AD). *J. Anthropol. Archaeol.* 32, 28–38.
- Killgrove, K., Montgomery, J., 2016. All Roads Lead to Rome: Exploring Human Migration to the Eternal City through Biochemistry of Skeletons from Two Imperial-Era Cemeteries (1st–3rd c AD). *PLoS ONE* 11, e0147585.
- Killgrove, K., Tykot, R.H., 2018. Diet and collapse: a stable isotope study of Imperial-era Gabii (1st–3rd centuries AD). *J. Archaeol. Sci.: Rep.* 19, 1041–1049.
- Kirwan, L.P., 1957. Rome beyond the southern Egyptian frontier. *Geogr. J.* 123, 13–19.
- Knudson, K.J., 2009. Oxygen isotope analysis in a land of environmental extremes: the complexities of isotopic work in the Andes. *Int. J. Osteoarchaeol.* 19, 171–191.
- Koch, P.L., Tuross, N., Fogel, M.L., 1997. The effects of sample treatment and diagenesis on the isotopic integrity of carbonate in biogenic hydroxylapatite. *J. Archaeol. Sci.* 24, 417–429.
- La Piana, G., 1927. Foreign groups in Rome during the first centuries of the Empire. *Harvard Theological Rev.* 20, 183–403.
- Law, R.C.C., 2009. The Garamantes and trans-Saharan enterprise in Classical times. *J. Afr. Hist.* 8, 181–200.
- Lebon, M., Müller, K., Bahain, J.-J., Frohlich, F., Falgueres, C., Bertrand, L., Sandt, C., Reiche, I., 2011. Imaging fossil bone alterations at the microscale by SR-FTIR microspectroscopy. *J. Anal. At. Spectrom.* 26, 922–929.
- Lenski, N., 2006. *Servi Publici* in Late Antiquity. In: Krause, J.-U., Witschel, C. (Eds.), *Die Stadt in der spätantike - Niedergang oder wacker? Verlag, Stuttgart*, pp. 335–357.
- Longin, R., 1971. New method of collagen extraction for radiocarbon dating. *Nature* 230, 241–242.
- Maaranen, N., Zakrzewski, S.R., Schutkowski, H., 2019. Hyksos in Egypt – utilising biodistance methods to interpret archaeological and textual evidence from Tell el-Dab'a. *Am. J. Phys. Anthropol.* 171, S69–S149.
- Maechler, M., Rousseeuw, P., Struyf, A., Hubert, M., Hornik, K., 2019. *cluster: Cluster Analysis Basics and Extensions*. R package version 2.1.0.
- Marado, L.M., Silva, A.M., 2016. The mandibular molar pit-tubercle (MMPT) dental nonmetric trait: Comprehensive analysis of a large sample. *HOMO* 67, 462–470.
- Martiniano, R., Caffell, A., Holst, M., Hunter-Mann, K., Montgomery, J., Müldner, G., McLaughlin, R.L., Teasdale, M.D., van Rheeën, W., Veldink, J.H., van den Berg, L. H., Hardiman, O., Carroll, M., Roskams, S., Oxley, J., Morgan, C., Thomas, M.G., Barnes, I., McDonnell, C., Collins, M.J., Bradley, D.G., 2016. Genomic signals of migration and continuity in Britain before the Anglo-Saxons. *Nat. Commun.* 7, 10326.
- Marzano, A., 2018. Fish and fishing in the Roman World. *J. Maritime Archaeol.* 13, 437–447.
- McArthur, J.M., 2001. Strontium isotope stratigraphy: LOWESS version 3: Best fit to the marine Sr-isotope curve for 0–509 Ma and accompanying look-up table for deriving numerical age. *J. Geol.* 109, 155–170.
- McLaughlin, R., 2014. *The Roman Empire and the Indian Ocean*. Pen & Sword, Barnsley.
- Mitteroecker, P., Gunz, P., 2009. Advances in geometric morphometrics. *Evol. Biol.* 36, 235–247.
- Moharrery, A., 2007. Effect of docking and energy of diet on carcass fat characteristics in fat-tailed Badghisian sheep. *Small Ruminant Res.* 69, 208–216.
- Moorrees, C.F.A., Fanning, E.A., Hunt, E.E., 1963. Age variation of formation stages for ten permanent teeth. *J. Dent. Res.* 42, 1490–1502.
- Nehlich, O., Richards, M.P., 2009. Establishing collagen quality criteria for sulphur isotope analysis of archaeological bone collagen. *Archaeol. Anthropol. Sci.* 1, 59–75.
- Nehlich, O., 2015. The application of sulphur isotope analyses in archaeological research: a review. *Earth Sci. Rev.* 142, 1–17.
- Nichol, C.R., 1990. *Dental Genetics and Biological Relationships of the Pima Indians of Arizona*. Arizona State University, Tempe.



- Nitsch, E.K., 2012. In: *Stable Isotope Evidence for Diet Change in Roman and Medieval Italy: Local, Regional and Continental Perspectives*. School of Archaeology, University of Oxford, Oxford, p. 352.
- Noy, D., 2000. *Foreigners at Rome: Citizens and Strangers*. Duckworth, London.
- O'Connell, T.C., Ballantyne, R.M., Hamilton-Dyer, S., Margaritis, E., Oxford, S., Pantano, W., Millett, M., Keay, S.J., 2019. Living and dying at the Portus Romae. *Antiquity* 93, 719–734. <https://doi.org/10.15184/aqy.2019.64>.
- Olsen, A.M., Westneat, M.W., 2015. StereoMorph: an R package for the collection of 3D landmarks and curves using a stereo camera set-up. *Methods Ecol. Evol.* 351–356.
- Passy, B.H., Robinson, T.F., Ayliffe, L.K., Cerling, T.E., Sponheimer, M., Dearing, M.D., Roeder, B.L., Ehleringer, J.R., 2005. Carbon isotope fractionation between diet, breath CO<sub>2</sub>, and bioapatite in different mammals. *J. Archaeol. Sci.* 32, 1459–1470.
- Peterson, B.J., Howarth, R.W., Garritt, R.H., 1985. Multiple stable isotopes used to trace the flow of organic matter in estuarine food webs. *Science* 227, 1361–1363.
- Pilloud, M.A., Maier, C., Scott, G.R., Edgar, H.J.H., 2018. Molar crenulation trait definition and variation in modern human populations. *HOMO* 69, 77–85.
- Prowse, T.L., 2001. In: *Isotopic and Dental Evidence for Diet from the Necropolis of Isola Sacra (1st-3rd centuries AD)*. Department of Anthropology, McMaster University, Hamilton, Italy, p. 356.
- Prowse, T., Schwarcz, H.P., Saunders, S., Macchiarelli, R., Bondioli, L., 2004. Isotopic paleodiet studies of skeletons from the Imperial Roman-age cemetery of Isola Sacra, Rome, Italy. *J. Archaeol. Sci.* 31, 259–272.
- Prowse, T.L., Schwarcz, H.P., Garnsey, P., Knyf, M., Macchiarelli, R., Bondioli, L., 2007. Isotopic evidence for age-related immigration to imperial Rome. *Am. J. Phys. Anthropol.* 132 (4), 510–519.
- Prowse, T.L., Saunders, S.R., Schwarcz, H.P., Garnsey, P., Macchiarelli, R., Bondioli, L., 2008. Isotopic and dental evidence for infant and young child feeding practices in an Imperial Roman skeletal sample. *Am. J. Phys. Anthropol.* 137, 294–308.
- Purcell, N., 1995. *Eating fish: the paradoxes of seafood*. In: Wilkins, J., Harvey, D., Dobson, M. (Eds.), *Food in Antiquity*. University of Exeter Press, Exeter, pp. 132–149.
- Reitsema, L.J., 2012. In: *Stable Carbon and Nitrogen Isotope Analysis of Human Diet Change in Prehistoric and Historic Poland*. Department of Anthropology, The Ohio State University, Columbus, p. 377.
- Rhine, S., 1990. Non-metric skull racing. In: Gill, G.W., Rhine, S. (Eds.), *Skeletal Attribution of Race*. Maxwell Museum of Anthropology, Albuquerque, pp. 9–20.
- Richards, M.P., Karavanić, I., Pettitt, P., Miracle, P., 2015. Isotope and faunal evidence for high levels of freshwater fish consumption by Late Glacial humans at the Late Upper Palaeolithic site of Sandalja II, Istria, Croatia. *J. Archaeol. Sci.* 61, 204–212.
- Rivollat, M., Mendisco, F., Pemonge, M.-H., Safi, A., Saint-Marc, D., Brémond, A., Couture-Veschambre, C., Rottier, S., Deguilloux, M.-F., 2015. When the waves of European Neolithization met: First palaeogenetic evidence from early farmers in the southern Paris Basin. *PLoS ONE* 10, e0125521.
- Roberts, S.B., Coward, W.A., Ewing, G., Savage, J., Cole, T.J., Lucas, A., 1988. Effect of weaning on accuracy of doubly labeled water method in infants. *Am. J. Physiol. - Regul., Integr. Comp. Physiol.* 254, R622–R627.
- Royer, A., Daux, V., Fourel, F., Lécuyer, C., 2017. Carbon, nitrogen and oxygen isotope fractionation during food cooking: Implications for the interpretation of the fossil human record. *Am. J. Phys. Anthropol.* 163, 759–771.
- Rutgers, L.V., van Strydonck, M., Boudin, M., van der Linde, C., 2009. Stable isotope data from the early Christian catacombs of ancient Rome: new insights into the dietary habits of Rome's early Christians. *J. Archaeol. Sci.* 36, 1127–1134.
- Salesses, K., 2015. In: *Archéo-biogéochimie isotopique, reconstitutions des régimes alimentaires et des schémas de mobilité, et interactions bio-culturelles. Les sépultures plurielles de la région X de la catacombe des Saints Pierre-et-Marcellin (Rome, I<sup>er</sup>-III<sup>e</sup> s. ap. J.-C.)*. Université de Bordeaux, Bordeaux, p. 352.
- Salesses, K., Dufour, É., Castex, D., Velemínský, P., Santos, F., Kucharová, H., Jun, L., Brůžek, J., 2013. Life history of the individuals buried in the St. Benedict cemetery (Prague, 15<sup>th</sup>-18<sup>th</sup> Centuries): insights from <sup>14</sup>C dating and stable isotope (δ<sup>13</sup>C, δ<sup>15</sup>N, δ<sup>18</sup>O) analysis. *Am. J. Phys. Anthropol.* 151, 202–214.
- Salesses, K., Dufour, E., Lebon, M., Wurster, C., Castex, D., Bruzek, J., Zazzo, A., 2014. Variability of bone preservation in a confined environment: the case of the catacomb of Sts Peter and Marcellinus (Rome, Italy). *Palaeogeogr. Palaeoclimatol. Palaeoecol.* 416, 43–54.
- Salesses, K., Fernandes, R., de Rochefort, X., Brůžek, J., Castex, D., Dufour, É., 2018. IsoArchEU: an open-access and collaborative isotope database for bioarchaeological samples from the Graeco-Roman world and its margins. *J. Archaeol. Sci.: Rep.* 19, 1050–1055.
- Salesses, K., Kaupová, S., Brůžek, J., Kuželka, V., Velemínský, P., 2019. An isotopic case study of individuals with syphilis from the pathological-anatomical reference collection of the national museum in Prague (Czech Republic, 19th century A.D.). *Int. J. Paleopathol.* 25, 46–55.
- Salesses, K., Fernandes, R., de Rochefort, X., Brůžek, J., Castex, D., Dufour, É., 2020. [www.IsoArchEU\(v.1.1\)](http://www.IsoArchEU(v.1.1)), (accessed 26/04/2020). <http://doi.org/10.17161/R31NJMTJ>.
- Schirmer, C., 2014. Food and status in ancient Rome: the evidence from literature. *Pithos* 13, 1–20.
- Schoeninger, M.J., DeNiro, M.J., Tauber, H., 1983. Stable nitrogen isotope ratios of bone collagen reflect marine and terrestrial components of Prehistoric human diet. *Science* 220, 1381–1383.
- Schotsmans, E.M.J., Toksoy-Köksal, F., Brettell, R.C., Bessou, M., Corbinau, R., Lingle, A.M., Bouquin, D., Blanchard, P., Becker, K., Castex, D., Knüsel, C.J., Wilson, A.S., Chapoulié, R., 2019. 'Not All That Is White Is Lime'—white substances from archaeological burial contexts: analyses and interpretations. *Archaeometry* 61, 809–827.
- Schrader, S.A., Buzon, M.R., Corcoran, L., Simonetti, A., 2019. Intraregional <sup>87</sup>Sr/<sup>86</sup>Sr variation in Nubia: new insights from the Third Cataract. *J. Archaeol. Sci.: Rep.* 24, 373–379.
- Scott, G.R., Irish, J.D., 2017. *Human Tooth Crown and Root Morphology: The Arizona State University Dental Anthropology System*. Cambridge University Press, Cambridge.
- Sellen, D.W., 2001. Comparison of infant feeding patterns reported for nonindustrial populations with current recommendations. *J. Nutr.* 131, 2707–2715.
- Sellen, D.W., 2007. Evolution of infant and young child feeding: implications for contemporary public health. *Annu. Rev. Nutr.* 27, 123–148.
- Sereno, P.C., Garcea, E.A.A., Jousse, H., Stojanowski, C.M., Saliège, J.-F., Maga, A., Ide, O.A., Knudson, K.J., Mercuri, A.M., Stafford Jr., T.W., Kaye, T.G., Giraudi, C., N'Siala, I.M., Cocca, E., Moots, H.M., Duthiel, D.B., Stivers, J.P., 2008. Lakeside cemeteries in the Sahara: 5000 Years of Holocene population and environmental change. *PLoS ONE* 3, e2995.
- Silver, M., 2016. Public slave in the Roman army: an exploratory study. *Ancient Soc.* 46, 203–240.
- Snowden Jr., F.M., 1947. The Negro in Classical Italy. *Am. J. Philol.* 68, 266–292.
- Spangenberg, J.E., Vennemann, T.W., 2008. The stable hydrogen and oxygen isotope variation of water stored in polyethylene terephthalate (PET) bottles. *Rapid Commun. Mass Spectrom.* 22, 672–676.
- Spurr, M.S., 1983. The cultivation of millet in Roman Italy. *Papers of the British School at Rome* 51, 1–15.
- Stark, R.J., 2017. Ancient lives in motion: a bioarchaeological examination of stable isotopes, nonmetric traits, and human mobility in imperial Roman context (1st-3rd c. CE). McMaster University, Hamilton.
- Stojanowski, C.M., Knudson, K.J., 2011. Biogeochemical inferences of mobility of early Holocene fisher-foragers from the Southern Sahara Desert. *Am. J. Phys. Anthropol.* 146, 49–61.
- Stojanowski, C.M., Knudson, K.J., 2014. Changing patterns of mobility as a response to climatic deterioration and aridification in the middle Holocene southern Sahara. *Am. J. Phys. Anthropol.* 154, 79–93.
- Tacoma, L.E., 2012. Number games. Quantifying immigrants in Rome, Moving Romans conference, Leiden, pp. 1-30.
- Tacoma, L.E., 2016. *Moving Romans : Migration to Rome in the Principate*. Oxford University Press, Oxford.
- Tafuri, M.A., Bentley, R.A., Manzi, G., di Lernia, S., 2006. Mobility and kinship in the prehistoric Sahara: strontium isotope analysis of Holocene human skeletons from the Acacus Mts. (southwestern Libya). *J. Anthropol. Archaeol.* 25, 390–402.
- Tafuri, M.A., Goude, G., Manzi, G., 2018. Isotopic evidence of diet variation at the transition between classical and post-classical times in Central Italy. *J. Archaeol. Sci.: Rep.* 21, 496–503.
- Team, R.C., 2020. R: A language and environment for statistical computing, URL <<https://www.R-project.org/>>.
- Thompson, A.H., Chaix, L., Richards, M.P., 2008. Stable isotopes and diet at Ancient Kerma, Upper Nubia (Sudan). *J. Archaeol. Sci.* 35, 376–387.
- Touzeau, A., Blichert-Toft, J., Amiot, R., Fourel, F., Martineau, F., Cockitt, J., Hall, K., Flandrois, J.-P., Lécuyer, C., 2013. Egyptian mummies record increasing aridity in the Nile valley from 5500 to 1500 yr before present. *Earth Planet. Sci. Lett.* 375, 92–100.
- Tsutaya, T., Yoneda, M., Abe, M., Nagaoka, T., 2019. Carbon, nitrogen, and sulfur stable isotopic reconstruction of human diet in a mountainous woodland village in Sendai in premodern Japan. *Anthropol. Sci.* 127, 131–138.
- Turchi, C., Buscemi, L., Previdere, C., Grignani, P., Brandstätter, A., Achilli, A., Parson, W., Tagliabracchi, A., Group, G.F.I., 2008. Italian mitochondrial DNA database: results of a collaborative exercise and proficiency testing. *Int. J. Legal Med.* 122, 199–204.
- van der Maaten, L., Hinton, G., 2008. Visualizing data using t-SNE. *J. Mach. Learn. Res.* 9, 2579–2605.
- Van Klinken, G.J., 1999. Bone collagen quality indicators for palaeodietary and radiocarbon measurements. *J. Archaeol. Sci.* 26, 687–695.
- Wang, Y., Cerling, T.E., 1994. A model of fossil tooth and bone diagenesis: implications for palaeodiet reconstruction from stable isotopes. *Palaeogeogr. Palaeoclimatol. Palaeoecol.* 107, 281–289.
- Warinner, C., Tuross, N., 2009. Alkaline cooking and stable isotope tissue-diet spacing in swine: archaeological implications. *J. Archaeol. Sci.* 36, 1690–1697.
- Webster, M., Sheets, H.D., 2010. *A Practical Introduction to landmark-based geometric morphometrics*. Paleontol. Soc. Pap. 16, 163–188.
- Weiss, A., 2004. *Sklave der Stadt: Untersuchungen zur öffentlichen Sklaverei in den Städten des Römischen Reiches*. Verlag, Stuttgart.
- Wilson, A., 2012. Saharan trade in the Roman period: short-, medium and long-distance trade networks. *Azania: Archaeol. Res. Africa* 47, 409–449.
- Wright, L.E., Schwarcz, H.P., 1998. Stable carbon and oxygen isotopes in human tooth enamel: identifying breastfeeding and weaning in Prehistory. *Am. J. Phys. Anthropol.* 106, 1–18.
- Wright, L.E., Schwarcz, H.P., 1999. Correspondence between stable carbon, oxygen and nitrogen isotopes in human tooth enamel and dentine: infant diets at Kaminaljuyú. *J. Archaeol. Sci.* 26, 1159–1170.
- Zazzo, A., 2014. Bone and enamel carbonate diagenesis: a radiocarbon prospective. *Palaeogeogr. Palaeoclimatol. Palaeoecol.* 416, 168–178.